

Living on the Edge: Unequal Rise of Global Population Exposure on Steep Terrain

Chakshu Gururani¹, Ugur Ozturk², and Thorsten Wagener¹

¹Institute for Environmental Science and Geography, University of Potsdam, Potsdam, Germany

²Department of Geography and Regional Research, University of Vienna, Vienna, Austria

Corresponding author: Chakshu Gururani (chakshu.gururani@uni-potsdam.de)

Keywords: landslide exposure; rapid urbanization; political instability

Competing interests: The authors declare no competing interests.

Author contributions: All authors designed the study. C.G. performed the analyses and drafted the manuscript. U.O. and T.W. provided guidance and edited the manuscript and figures.

This manuscript is a non-peer reviewed preprint submitted to EarthArXiv.

Compiled on April 29, 2026.

Abstract

The global population living on steep terrain is rising, so is their landslide risk. However, hotspots and driving mechanisms of increasing exposure remain poorly understood. We assess changes in global gridded population and settlement characteristics on steep terrain ($\geq 10^\circ$ hillslope inclination) aggregated over topographic catchments (mean area $\sim 10,000$ km²) for 1975–2025. We find that about 341 million additional people now live on steep terrain, increasing the total from 494 to 835 million. The strongest growth occurred in tropical catchments, commonly in peri-urban areas, indicating that exposure is increasingly forming in rapidly expanding settlement fringes. More than half of this growth occurred in low- and lower-middle-income countries. Hence, further exacerbating those countries' global socio-economic disadvantage, exposure is rising in places with strained planning and response capacity. Our results provide a global baseline identifying priority regions for hazard monitoring and risk-informed planning.

Global population exposed to natural hazards roughly doubled from about 1.9 to 4 billion between 1975 and 2015 [1]. Aside from this natural increase, today nearly 90 million, three-quarters of all displaced people live in regions classified as highly or extremely hazard-prone [2, 3]. Much of this movement occurs in the tropics [2], where limited data constrains evaluating the physical risks people face [4, 5]. Thus, displacement grows in regions where hazard information is limited, and where quantification of exposure to hazards is poor, especially on steep and unstable terrain [6].

While progress has been made in assessing exposure to major hazards such as floods or tropical cyclones, multiple IPCC reports highlight global landslide assessments to be often limited to coarse scales [7, 8]. Exposure to landslides remains one of the least explored risks at global scales, due to three related reasons. (i) Impacts are usually recorded only after major events

[9, 10, 11], which tend to capture damage only in well-studied or more populated areas. (ii) Many global studies rely heavily on inventories or case-specific observations [12, 13]. (iii) Limited data cripples global assessments and models. As a result, landslides are rarely included in global multi-hazard risk assessments that increasingly explore how climate extremes and hazard exposure are changing [14, 15].

Several recent studies have advanced global and national assessments of landslide exposure, but none explicitly tracks how exposure evolves as populations and settlements redistribute across steep terrain. National income and land-cover change have been shown to govern landslide impacts at the country scale, without resolving local settlement patterns or sub-national variation in exposure [16]. Exposure to large, slow-moving, deep-seated landslides in cities has more than doubled since 1985 [17], leaving open how this exposure varies by settlement type. “Slope climbing” in global urban expansion has been quantified [18], showing that cities increasingly expand onto steeper slopes, yet how this pattern extends to population growth on steep terrain in rural and peri-urban settings remains to be explored. Valuable global exposure estimates exist for rainfall-triggered landslides between 2001–2019, by linking modelled hazard and population [19]. However, this snapshot does not trace how exposure changes over time.

Both physical and human systems are changing, shifting locations where landslide instability intersects with population growth [20]. Rainfall extremes are intensifying in many regions [21, 22], which can change and expand the areas prone to rainfall-triggered landslides [23, 24, 25, 26]. In parallel, settlement growth is pushing into steeper terrain through land-use change [27], deforestation [28] and the expansion of both formal and informal settlements [29, 30]. Differences in income, infrastructure and governance influence settlement choices, safety standards, and the capacity to adapt [31, 8]. As a result, landslide exposure is changing.

Although global landslide exposure is increasingly discussed, its dynamics remain under-explored especially below country scale. We use topographically defined catchments as a helpful unit to aggregate hillslope processes and to not be defined by political, but natural boundaries. Two critical questions arise: where is population growth occurring on steep terrain ($\geq 10^\circ$) and which settlement types, for example urban centres, peri-urban areas or rural settlements, are most affected across regions? We address these questions by analysing steep-slope population exposure from 1975–2025 at the HydroBASINS Level 5 catchment scale (mean area $\sim 10,000$ km²) [32]. We use steepness as a globally consistent proxy for landslide-prone terrain, defining steep terrain as areas with slope $\geq 10^\circ$. This threshold is commonly used in landslide studies and is representative of conditions where rainfall-triggered landslides occur frequently [e.g., 30, 33, 34]. We then link population exposure change to settlement expansion, climate zones, income levels and political stability. Our approach complements recent global studies on landslide exposure while adding a multi-decadal view of where steep-slope exposure increased and under which development contexts.

Results

Rising fast on steep ground: Tropical climates dominate steep-slope population growth

Steep terrain and rapid population growth converge in several climate zones. We use the 1 km gridded population and settlement data from the Global Human Settlement Layer (GHSL) datasets [35, 36] and climate zones from the IPCC Climate Zone Map, derived from long-term monthly temperature and precipitation data (1901–2019) [37]. Population growth on steep terrain is heterogenous across mountain belts, but concentrated in discrete regional clusters (Figure 1). Several of these clusters are in regions that are inconsistently highlighted in event-

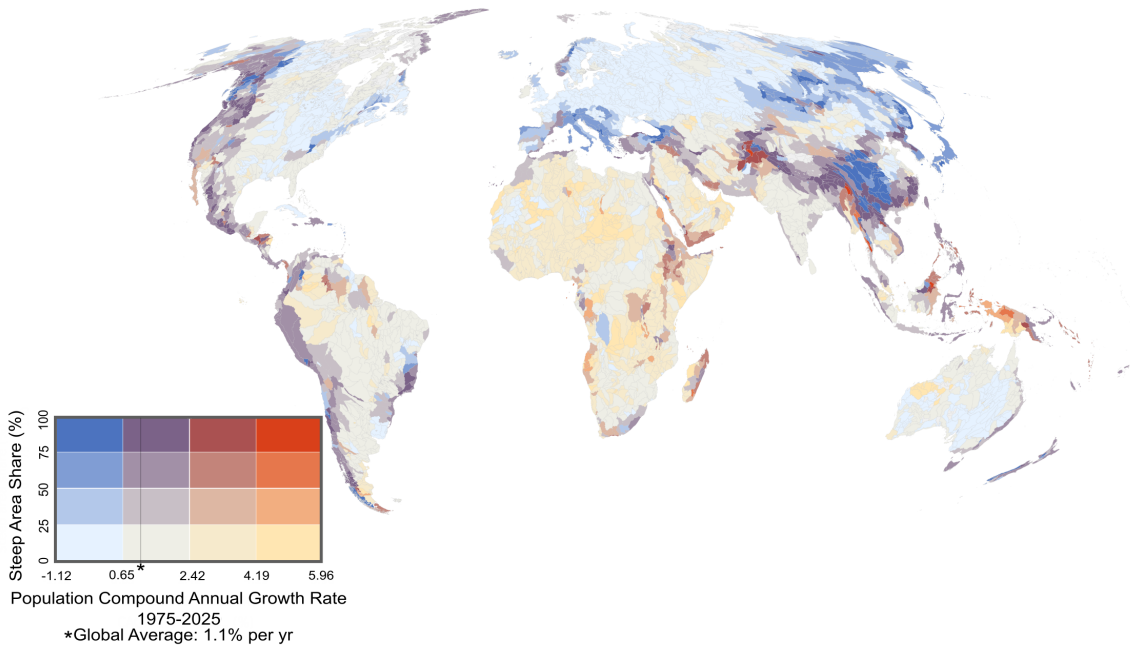


Figure 1: Population growth on steep terrain, 1975–2025. Bivariate map showing the population Compound Annual Growth Rate (CAGR; x-axis of legend) and the share of each catchment classified as steep ($\geq 10^\circ$; y-axis of legend) between 1975 and 2025. Reddish hues indicate catchments with both high steep-slope share and high population growth.

based global assessments, such as the Ethiopian Highlands and the Southern Levant [9, 12].

We find the highest Compound Annual Growth Rates (CAGR) of steep-slope population in tropical montane regions ($\sim 2.3\% \text{ yr}^{-1}$), increasing from 42 million people in 1975 to 128 million in 2025. Tropical wet ($\sim 1.9\% \text{ yr}^{-1}$) and dry ($\sim 1.8\% \text{ yr}^{-1}$) climates also have growth rates higher than the global average ($\sim 1.1\% \text{ yr}^{-1}$), with populations on steep terrain rising from 28 to 70 million and from 16 to 39 million, respectively. In absolute terms, the largest additions to steep-terrain population occurred in tropical montane (+86 million), followed by warm temperate dry (+68 million) and tropical moist (+61 million). Although the global population share living on steep terrain decreases slightly (from 12% in 1975 to 10.2% in 2025), the absolute number increases substantially (from 495 to 835 million, +340 million).

Rapid urbanization is reshaping where people live

To better understand this process on steep terrain, we quantified how the population living on steep terrain is distributed across the seven GHS-SMOD settlement classes (including urban center, peri-urban, etc.) between 1975 and 2025 (Figure 2) (see Materials for details). Steep-slope population growth in terms of absolute numbers was the largest in Sub-Saharan Africa (+98 million) and East Asia & the Pacific (+82 million), followed by Latin America and the Caribbean (+58 million) and South Asia (+50 million), while Europe (+1 million) and North America (+4 million) changed only modestly.

Our results show a shift of steep-slope population towards peri-urban and urban classes between 1975 and 2025. Globally, peri-urban steep-slope population increased from 70 million to 179 million (+109 million), and urban-centre steep-slope population increased from 68 million to



Figure 2: Change in population distribution across settlement classes in steep areas (with $\geq 10^\circ$ slope), 1975–2025. The figure shows steep population shares across GHS-SMOD settlement classes. Most regions show increasing shares in peri-urban and urban classes over time, with notable rural-to-urban transitions in Sub-Saharan Africa and East Asia & the Pacific. The full 5-year stepwise transitions is shown in Supplement S3.

183 million (+115 million). The peri-urban shift is strongest in South Asia and Sub-Saharan Africa, where the share of steep-slope population living in peri-urban regions more than doubled, from 15% to 31% and from 13% to 32%, respectively. Over the same period, the share of global population in very low-density rural areas decreased from 9% to 5%. We also analysed change in the steep area shares of these settlement classes and found the highest increases in steep-area share for peri-urban and semi-dense urban classes in several regions (Supplement S1). This pattern of outward expansion into steeper terrain is consistent with the concept of ‘slope climbing’ observed in global urban expansion [18], as well as with documented shifts into peripheral and adjacent mountain areas [17], often via informal peri-urban growth on potentially unstable steep slopes [38, 29].

Living on the edge: Global distribution of steep-slope population change

Low- and lower-middle-income countries account for about 56% of population growth on steep terrain between 1975 and 2025. Using the latest World Bank income-group classification, our results show that the population on steep terrain only grew by about 114 million in lower-middle-income countries and by about 83 million in low-income countries. Over the same period, steep-slope population grew by about 10 million in high-income countries, and by about 61 million in other or unclassified countries. Moreover, low-income countries have the highest share of the total population living on steep terrain in 2025 (18%). The lowest share across all income groups belongs to high-income countries at 6.4% (Supplement Figure S6).

The growth of population living on steep terrain coincides with politically fragile regions. The top 10 hotspots identified in our analysis, those with the largest absolute increases in population living on steep hillslopes, are located in low- or lower-middle-income countries (Figure 3). Many are in countries that rank near the bottom on the World Bank ‘Political Stability and Absence of Violence’ index (Supplement S4). The index reflects perceptions of the likelihood of political instability and politically motivated violence, including terrorism. It is reported for each country as a rank from 1 to 100, where 1 indicates the lowest stability and 100 the highest.

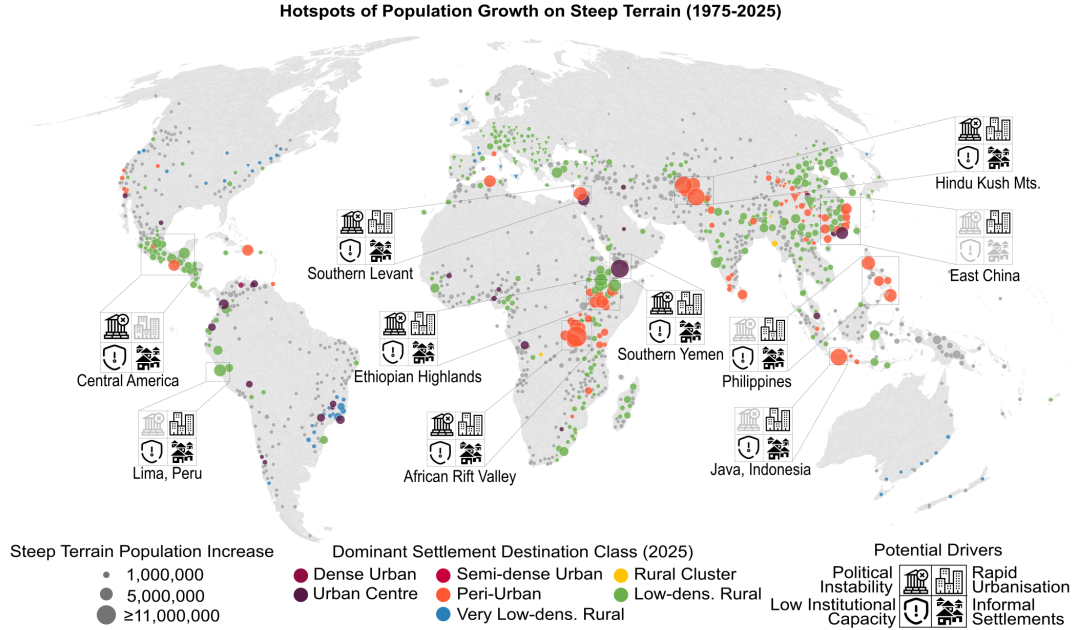


Figure 3: Steep-slope population change and dominant settlement patterns, 1975–2025. Map shows the absolute increase in population living on steep terrain ($\geq 10^\circ$) by 2025 per catchment, with point size scaled to total growth and colour indicating the dominant GHS-SMOD settlement class in 2025. Labeled hotspots highlight where steep-slope exposure intersects with different settlement patterns and contextual drivers including political instability (Supplement Figure S4), low institutional capacity, rapid urbanisation and informal settlement expansion (Definitions provided in Supplement S5). Contextual drivers, excluding political instability, are based on regional landslide risk studies in those hotspots provided in Supplement S6. Extracted from published case studies, contextual drivers may not represent the entirety of the study period. Inverted triangles represent population decrease on steep terrain.

Steep-slope population growth hotspots are not only shaped by terrain and settlement change but also frequently occur in contexts with limited institutional capacity to manage risk. The largest single increase in steep-slope population occurred in the region surrounding Lake Kivu (tropical montane, low-income), where about 10 million additional people moved onto steep terrain in a single catchment (1975–2025) (Figure 3). This region lies on the western flank of the East African Rift valley and experiences frequent landslides [39]. It is also marred by political instability [28]. Several other hotspots saw population growth of 6 to 8 million people on steep slopes, including southern Yemen (+7.5 million), the Hindu Kush region (+7 million), and Java, Indonesia (+6.37 million). These countries also rank consistently low in political stability, including Yemen (rank 1), Pakistan (rank 7), Ethiopia (rank 6) and Burundi (rank 13) (Supplement S4).

Discussion

Steep-slope exposure is growing fastest in low-income, peri-urban regions with high hazard research potential

Our findings show that about 198 million of the 341 million additional people on steep hillslopes (1975–2025) live in low- and lower-middle-income countries. The largest population increases were found in tropical climates, mainly in Asia, Africa and South America. Large parts of these

continents remain poorly investigated in landslide-climate research [20] or any other natural-hazard research [4, 5], despite increasing severity of future climate conditions, such as more frequent rainfall extremes [21, 24]. Hence, the areas experiencing the greatest population growth on steep terrain often overlap with those expected to experience more landslide-triggering events. We visualize these interactions in causal loop diagram (Figure 4) that links the formation of steep-slope exposure to physical constraints and limited institutional capacity to enforce urban planning.

The largest population increase on steep terrain aligns with rapid peri-urban and semi-dense urban expansion (Supplement S1). The share of the population living on steep terrain in peri-urban areas more than doubled in Sub-Saharan Africa (from 13% to 32%) and South Asia (from 15% to 31%) between 1975 and 2025. Peri-urban zones are often characterized by limited land-use control, stretched infrastructure, and weak enforcement [40]. In high-income regions, where planning capacity and flat land availability are greater, peri-urban growth is modest and shows little engagement with steep terrain. These patterns reinforce evidence that exposure is forming most rapidly precisely where monitoring infrastructure, hazard planning, research and reporting systems are most strained [5].

Urban sprawl is known to disproportionately affect lower-income households and vulnerable communities, who are more likely to occupy hazardous land with limited planning oversight globally [41, 40]. Unsurprisingly, the vast majority (up to 80%) of landslide deaths are concentrated in poor, informal settlements [e.g., 42, 38]. Several regional analyses confirm our findings locally in rapidly growing cities like Lima, Peru [43], São Paulo, Brazil [44], Medellín, Columbia [38], Bujumbura, Burundi [45], Freetown, Sierra Leone, Antipolo and Baguio, the Philippines, Port-au-Prince, Haiti [30]. All documenting outward peri-urban expansion in areas with limited land-use regulation.

Global risk assessments can miss key hotspots due to incomplete or inconsistent impact data

For example, the Kivu Rift region, which is one of the hotspots identified in our analysis (Figure 3), is also recognized as a landslide hotspot in several regional studies [e.g., 39, 28]. However, it is not classified as a high-landslide-mortality risk hotspot in global analyses using the EM-DAT Disaster Database [9]. Limitations of EM-DAT due to reporting gaps have been widely reported [46, 11]. Moreover, we observed an increase of 60 million people living on steep terrain in regions that are not classified by the World Bank's income groups, such as the Ethiopian highlands. Thus, despite strong local evidence [16], global assessments can be limited by the availability and consistency of underlying event data [13]. We bypassed this data limitation by using a steepness-based threshold to identify steep terrain instead [e.g., 30, 33]. Steepness should therefore be interpreted as a screening indicator. The slope-threshold approach is most informative where steepness constrains settlement and where peri-urban growth extends into steeper ground. Although steepness is the primary control of landslides [47], it is less informative where instability is dominated by geology, soils, land cover, drainage, or engineered slope modification [48, 49, 50, 51]. In these settings, exposure can increase without a comparable change in the likelihood of hazard. However, our core conclusions are robust and provide a first-order analysis that can be refined with additional data: the share of the exposed population declines for all income groups as the slope threshold is tightened, but differences across income groups persist (Slope-threshold sensitivity assessment in Supplement S8), indicating that the pattern is not driven by a single cutoff.

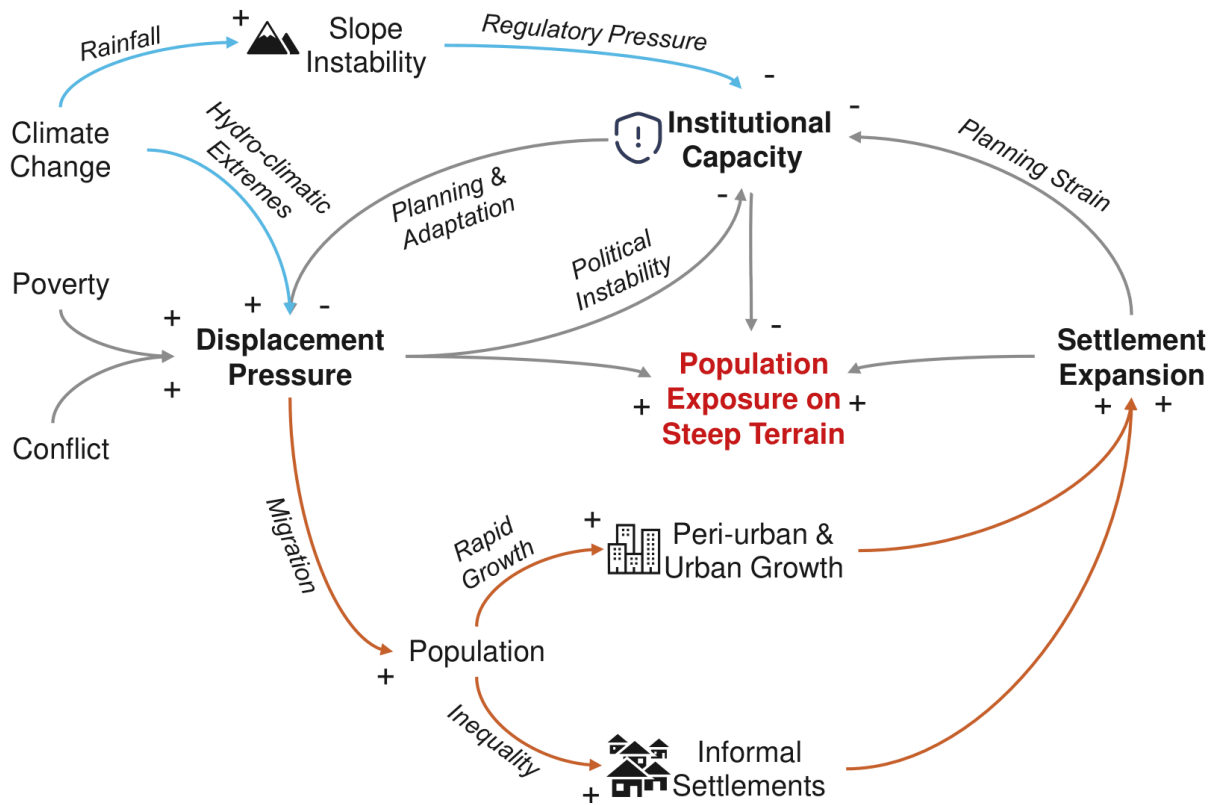


Figure 4: Causal loop diagram of interacting drivers of population exposure on steep terrain. Bold variables denote the core processes central to this study, surrounding factors provide context. Arrows indicate causal links. (+)/(-) denote positive and negative effects. The blue pathways represent climatic controls on slope instability and displacement, while the brown pathways represent population and settlement processes driving expansion. The diagram is simplified depiction of cases based on the definitions provided in Supplement S5 for each identified hotspot in Figure 3.

Regions with the fastest-growing steep-slope population often face multiple challenges, with landslides being only one among them

Some hotspots in the Hindu Kush Mountains, the Kivu Rift, South-East Asia, and parts of Central America, also face compounding pressures, including multi-hazard risks, conflict, political instability, land scarcity, and displacement [3, 2]. Hence, most lie in countries ranking at the bottom of the World Bank’s ‘Political Stability and Absence of Violence’ index,

There is growing evidence in literature relating climate hazards to increased conflict over access to resources, serving as a catalyst for violence [52, 53]. In these socially fragile environments, slope-related hazards are rarely the most immediate concern between urgent, overlapping threats of violence, displacement and food insecurity. These concerns shape settlement decisions more than geomorphological risks alone [28, 54].

Slope-instability exposure often results from limited alternatives during a crisis, rather than from deliberate settlement in hazardous areas (Figure 3). In the African Rift Valley, cities like Bujumbura and Bukavu have expanded rapidly and informally into unstable terrain, amid ongoing political instability, displacement and limited planning capacity [28, 55, 56]. In the Ethiopian Highlands, steep slopes coincide with high population growth, erratic rainfall and limited flat land, while livelihoods remain heavily dependent on increasingly climate-sensitive agriculture [57, 58, 59]. In southern Yemen, conflict, repeated flash floods and institutional

breakdown have pushed millions into informal settlements on unstable slopes, where hazard monitoring and land governance are weak [60, 61]. In the Hindu Kush region of Afghanistan and northern Pakistan, populations face multiple hazards [9, 62]. People are often forced to live on steep terrain due to conflict, land scarcity and the absence of basic infrastructure or emergency response [63, 64, 65]. But significant change does not just occur in conflict-ridden regions with poor governance. The eastern coast of China proves to be a contrasting case, where steep-terrain exposure is increasing alongside rapid development and institutional capacity. Recent studies show that climate change is increasing landslide risk in China by intensifying rainfall extremes and shifting precipitation patterns that can trigger slope failures [25], while rapid urbanization and infrastructure expansion are increasing exposure [66] and the value of assets at risk [67, 68]. (Full cases in the Supplement S6).

We show that in most hotspots, exposure on steep slopes is increasing where rapid settlement expansion intersects with broader socioeconomic and environmental constraints. Thus, inequality shapes not only who is affected by the hazard, but also where exposure is forming. The implication is clear: future landslide risk will be shaped disproportionately in a small set of fast-changing, lower-income tropical and mid-latitude regions. Research priorities should lie in Sub-Saharan Africa and South Asia, including the Kivu Rift, parts of the Ethiopian Highlands, and the Hindu Kush region, where growth on steep slopes can even exceed that on flatter ground (Supplement S2). We recommend focusing investment on hazard and impact data, on monitoring and institutional capacity and on understanding how settlement expansion drives exposure on steep slopes. Increasing exposure to steep landslide-prone terrain should be treated as a sustainable development concern as much as a hazard concern [69, 70].

Materials

Spatial units and aggregation

We selected topographic catchments as the primary spatial units. They represent natural boundaries for hillslope processes and reduce artifacts introduced by political borders. We choose to operate at the HydroBASINS Level 5 catchment scale, which provides global polygon boundaries for medium-sized catchments (10,000 km² mean area) derived from HydroSHEDS flow accumulation data using hierarchical Pfafstetter coding [32].

We aligned all gridded datasets to a common 1 km analysis grid by nearest neighbour method to avoid altering original data artificially. We then aggregated pixel-level values to catchments by summing population counts and computing settlement class shares within each catchment. Key aggregation assumptions were: (i) gridded population represents average conditions within each pixel, and (ii) catchment-scale summaries capture broad exposure patterns while smoothing local heterogeneity.

Datasets

We quantified long-term population and settlement dynamics using the Global Human Settlement Layer (GHSL). We used population counts from GHS-POP [1975–2025, 1 km resolution, 5-year intervals; 35], chosen for its long temporal coverage, uniform methodology and compatibility with other GHSL products used in this study. The dataset redistributes census-based population counts onto a grid using built-up information for global comparability.

We characterised settlement structure using GHS-SMOD [(Settlement Model, 1975–2025, 1 km resolution; 36]. GHS-SMOD is produced within the same GHSL framework as GHS-POP, al-

lowing joint analysis of population and settlement change on a common grid. GHS-SMOD classifies each grid cell into settlement categories based on the Degree of Urbanisation (DEGURBA) framework endorsed by the UN Statistical Commission. DEGURBA integrates population density, built-up density and spatial contiguity to produce globally comparable settlement classes. GHS-SMOD classes used in this study are urban centre, dense urban, semi-dense urban, peri-urban, rural cluster, low-density rural and very low-density rural.

We assigned each catchment a climate zone using the IPCC Climate Zone Map [2019; 37]. This gridded dataset applies a standardized classification scheme to Climate Research Unit Time Series (CRU TS) monthly temperature and precipitation data [1901–2019; 71], defining 12 domains based on thermal (polar, boreal, cool temperate, warm temperate, tropical), moisture (wet, moist, dry) and elevation (montane) regimes. We used this classification because it provides a compact set of global climate domains that supports clear cross-region comparison. The dataset contains 12 climate classes: Tropical Montane, Tropical Wet, Tropical Moist, Tropical Dry, Warm Temperate Moist, Warm Temperate Dry, Cool Temperate Moist, Cool Temperate Dry, Boreal Moist, Boreal Dry, Polar Moist and Polar Dry. We labelled each catchment by the dominant climate class within its boundary. This approach assumes that catchments with mixed climate coverage can be represented by their dominant class. Mixed-climate catchments therefore introduce some boundary uncertainty. Alternative climate classifications are possible, for example Köppen–Geiger, but the IPCC classification uses fewer classes and is better suited to the broad comparative focus of our analysis and compatibility of our results with future IPCC reports.

We used the latest World Bank Income Classification [2024; 72] to represent socioeconomic differences, assigning countries to low-, lower-middle-, upper-middle- or high-income groups. This classification provides a consistent global grouping for comparing exposure patterns. The 2024 classification used here includes 27 low-income, 55 lower-middle-income, 55 upper-middle-income and 61 high-income countries. We attributed each catchment to an income group using a population-weighted dominant-country approach. Specifically, we identified the country contributing most to the catchment’s steep-slope population change and assigned that country’s income group to the catchment.

To characterise institutional stability and conflict exposure in regions experiencing rapid steep-slope population growth, we used the World Bank Worldwide Governance Indicators (WGI), specifically the Political Stability and Absence of Violence/Terrorism percentile rank (1996–2024) [73]. In this metric, lower ranks indicate lower political stability across countries. We linked WGI rankings to catchments using the same population-weighted dominant-country approach as above to ensure consistency with the income-group attribution.

Terrain steepness and definition of ‘steep’

Terrain steepness was obtained from GEOMORPHO90’s 250m slope layers [74], derived from the globally consistent and hydrologically conditioned MERIT-DEM [75]. We selected GEOMORPHO90 over other raw terrain products because it provides a standardised, corrected surface suitable for our analysis. Although 90m layers are available as supplemental products, we used the 250m release because it is the primary global distribution with uniform preprocessing. We conducted the analysis at 1 km because a global, multi-decadal workflow at this resolution provides an efficient compromise that captures broad exposure patterns, while still being computationally feasible. We resampled the slope layer to 1 km using maximum aggregation, ensuring that steep terrain was preserved when matching the GHSL grid.

We defined steep terrain as slope $\geq 10^\circ$, a threshold widely used in landslide studies and representative of conditions where rainfall-triggered landslides occur frequently [e.g., 30, 33, 34].

We calculated steep-slope population by masking the population rasters to pixels with slope $\geq 10^\circ$ and summing within each catchment.

Robustness and sensitivity analyses

We assessed slope-threshold sensitivity by repeating key analyses using alternative slope thresholds (8° , 10° , 12° and 15°) to evaluate how results depend on the definition of ‘steep’ (Supplement S8). As expected, the exposed share declines for all income groups as the threshold is tightened. However, the ranking and separation between groups remain similar across thresholds. Hence, the income-group pattern is unbiased by the specific choice of the cutoff.

We assessed robustness to population data choice by repeating our steep-slope population growth analysis with WorldPop and comparing it with GHS-POP over the overlap period 2000–2020. We measured agreement between the two datasets by correlating the catchment rankings of positive steep-slope population growth, using Spearman’s ρ (slope $\geq 10^\circ$). We obtained a rank correlation of $\rho = 0.79$, indicating similar identification of high-growth catchments despite differences in population modelling inputs and methods. We also compared hotspot overlap using the top-50 catchments by positive steep-slope growth: 40 catchments overlapped, with 10 WorldPop-only and 10 GHS-only catchments in the Top-50 set.

In map comparisons (Supplement S7), the non-overlapping catchments typically occur in the same broader hotspot regions (in the neighbourhood) of overlapping catchments. This pattern suggests both datasets identify similar hotspot regions, while differences remain in the exact catchment ranking. These disagreements are consistent with known differences in gridded population modelling and input data between products [54], for example census harmonisation, redistribution or allocation methods, which can shift population totals across adjacent catchments. These differences can shift population totals across adjacent catchments and affect Top-N rankings, but they do not alter the main hotspot patterns identified in this study.

Software and Implementation

All data processing and analysis were performed using Python 3.12.3.

Acknowledgement

CG and TW acknowledge support from the Alexander von Humboldt Foundation in the framework of the Alexander von Humboldt Professorship endowed by the German Federal Ministry of Education and Research (BMBF). UO is funded by the European Union (ERC, UrbanSlide, Grant 101160656, Doi: 10.3030/101160656). Views and opinions expressed are, however, those of the author(s) only and do not necessarily reflect those of the European Union or the European Research Council. Neither the European Union nor the granting authority can be held responsible for them.

References

- [1] M. Pesaresi, D. Ehrlich, T. Kemper, A. Siragusa, A. Florczyk, S. Freire, and C. Corban. Atlas of the Human Planet 2017: Global Exposure to Natural Hazards. Technical Report KJ-NA-28556-EN-N (online), KJ-NA-28556-EN-C (print), KJ-NA-28556-EN-E (ePub), Joint Research Centre, Luxembourg (Luxembourg), 2017.

- [2] IDMC. Global Report on Internal Displacement. Technical report, Internal Displacement Monitoring Centre, 2025.
- [3] UNHCR. No Escape II: The Way Forward. Bringing climate solutions to the frontlines of conflict and displacement. Technical report, United Nations High Commissioner for Refugees, 2025. URL <https://www.unhcr.org/media/no-escape-ii-way-forward>.
- [4] Adam Emmer. Geographies and Scientometrics of Research on Natural Hazards. *Geosciences* 2018, Vol. 8, Page 382, 8(10):382, 10 2018. ISSN 2076-3263. doi: 10.3390/GEOSCIENCES8100382. URL <https://www.mdpi.com/2076-3263/8/10/382/htmhttps://www.mdpi.com/2076-3263/8/10/382>.
- [5] Lina Stein, S. Karthik Mukkavilli, Birgit M. Pfitzmann, Peter W.J. Staar, Ugur Ozturk, Cesar Berrospi, Thomas Brunschwiler, and Thorsten Wagener. Wealth Over Woe: Global Biases in Hydro-Hazard Research. *Earth's Future*, 12(10):e2024EF004590, 10 2024. ISSN 23284277. doi: 10.1029/2024EF004590;REQUESTEDJOURNAL:JOURNAL:23284277;PAGE:STRING:ARTICLE/CHAPTER. URL </doi/pdf/10.1029/2024EF004590https://onlinelibrary.wiley.com/doi/abs/10.1029/2024EF004590https://agupubs.onlinelibrary.wiley.com/doi/10.1029/2024EF004590>.
- [6] Joaquin V. Ferrer, Guilherme Samprogna Mohor, Olivier Dewitte, Tomáš Pánek, Cristina Reyes-Carmona, Alexander L. Handwerker, Marcel Hürlimann, Lisa Köhler, Kanayim Teshebaeva, Annegret H. Thieken, Ching Ying Tsou, Alexandra Urgilez Vinueza, Valentino Demurtas, Yi Zhang, Chaoying Zhao, Norbert Marwan, Jürgen Kurths, and Oliver Korup. Human Settlement Pressure Drives Slow-Moving Landslide Exposure. *Earth's Future*, 12(9):e2024EF004830, 9 2024. ISSN 23284277. doi: 10.1029/2024EF004830. URL </doi/pdf/10.1029/2024EF004830https://onlinelibrary.wiley.com/doi/abs/10.1029/2024EF004830https://agupubs.onlinelibrary.wiley.com/doi/10.1029/2024EF004830>.
- [7] Christopher B Field, V R Barros, K J Mach, M D Mastrandrea, M Van Aalst, W N Adger, D J Arent, J Barnett, R Betts, and T E Bilir. Technical summary Climate Change 2014: Impacts, Adaptation, and Vulnerability. Part A: Global and Sectoral Aspects. Contribution of Working Group II to the Fifth Assessment Report of the Intergovernmental Panel on Climate Change ed CB Field et al. *Climate Change*, 2014:35–94, 2014.
- [8] Michael Oppenheimer, Maximiliano Campos, Rachel Warren, Joern Birkmann, George Luber, Brian O'Neill, Kiyoshi Takahashi, and M Brklacich. Emergent risks and key vulnerabilities Climate Change 2014: Impacts, Adaptation, and Vulnerability. Part A: Global and Sectoral Aspects. Contribution of Working Group II to the Fifth Assessment Report of the Intergovernmental Panel on Climate Change ed CB Field et al. *Cambridge UK, and New York: [sn]*, 2014.
- [9] M Dilley, R S Chen, U Deichmann, A Lerner-Lam, M Arnold, J Agwe, P Buys, O Kjekstad, Bradfield Lyon, and Greg Yetman. Natural disaster hotspots: A global risk analysis. *World Bank Disaster Risk Management Series*, 5:1–132, 11 2005. doi: 10.1007/978-3-322-82113-3{\-}1.
- [10] Melanie J. Froude and David N. Petley. Global fatal landslide occurrence from 2004 to 2016. *Natural Hazards and Earth System Sciences*, 18(8):2161–2181, 8 2018. ISSN 16849981. doi: 10.5194/NHESS-18-2161-2018.
- [11] Damien Delforge, Valentin Wathelet, Regina Below, Cinzia Lanfredi Sofia, Margo Tonnelier, Joris A.F. van Loenhout, and Niko Speybroeck. EM-DAT: the Emergency Events Database. *International Journal of Disaster Risk Reduction*, 124:105509, 6 2025. ISSN

- 2212-4209. doi: 10.1016/J.IJDRR.2025.105509. URL <https://www.sciencedirect.com/science/article/pii/S2212420925003334?via%3Dihub>.
- [12] Farrokh Nadim, Oddvar Kjekstad, Pascal Peduzzi, Christian Herold, and Christian Jaedicke. Global landslide and avalanche hotspots. *Landslides* 2006 3:2, 3(2):159–173, 2 2006. ISSN 1612-5118. doi: 10.1007/S10346-006-0036-1. URL <https://link.springer.com/article/10.1007/s10346-006-0036-1>.
- [13] Seçkin Fidan, Hakan Tanyaş, Abdullah Akbaş, Luigi Lombardo, David N. Petley, and Tolga Görüm. Understanding fatal landslides at global scales: a summary of topographic, climatic, and anthropogenic perspectives. *Natural Hazards* 2024 120:7, 120(7):6437–6455, 2 2024. ISSN 1573-0840. doi: 10.1007/S11069-024-06487-3. URL <https://link.springer.com/article/10.1007/s11069-024-06487-3>.
- [14] Tayler A. Schillerberg and Di Tian. Global Assessment of Compound Climate Extremes and Exposures of Population, Agriculture, and Forest Lands Under Two Climate Scenarios. *Earth’s Future*, 12(9):e2024EF004845, 9 2024. ISSN 2328-4277. doi: 10.1029/2024EF004845. URL </doi/pdf/10.1029/2024EF004845https://onlinelibrary.wiley.com/doi/abs/10.1029/2024EF004845https://agupubs.onlinelibrary.wiley.com/doi/10.1029/2024EF004845>.
- [15] Zélie Stalhandske, Marleen C. de Ruiter, Jonathan Chambers, Sandra Zimmermann, Felipe J. Colón-González, Nivedita Sairam, David N. Bresch, and Chahan M. Kropf. Global assessment of population exposure to multiple climate-related hazards from 2003 to 2021: a retrospective analysis. *The Lancet Planetary Health*, 9(8):101295, 8 2025. ISSN 2542-5196. doi: 10.1016/J.LANPLH.2025.101295. URL <https://www.sciencedirect.com/science/article/pii/S2542519625001731?via%3Dihub#sec2>.
- [16] Seçkin Fidan, Tolga Görüm, Abdullah Akbaş, Bikem Ekberzade, and Ugur Ozturk. Wealth and land-cover change govern landslide fatalities on world’s mountains. *Science Advances*, 12(15):eaec2739, 2026.
- [17] Joaquin V. Ferrer, Cassiano Bastos Moroz, Selin Yüksel, Olivier Dewitte, Karen Lebek, Norbert Marwan, Jürgen Kurths, and Oliver Korup. Exposure to Large Landslides in Cities Outpaces Urban Growth. *Geophysical Research Letters*, 52(15):e2025GL115170, 8 2025. ISSN 1944-8007. doi: 10.1029/2025GL115170. URL </doi/pdf/10.1029/2025GL115170https://onlinelibrary.wiley.com/doi/abs/10.1029/2025GL115170https://agupubs.onlinelibrary.wiley.com/doi/10.1029/2025GL115170>.
- [18] Kaifang Shi, Yuanzheng Cui, Shirao Liu, and Yizhen Wu. Global Urban Land Expansion Tends To Be Slope Climbing: A Remotely Sensed Nighttime Light Approach. *Earth’s Future*, 11(4):e2022EF003384, 4 2023. ISSN 23284277. doi: 10.1029/2022EF003384;WEBSITE:WEBSITE:AGUPUBS;WGROU:STRING: PUBLICATION. URL </doi/pdf/10.1029/2022EF003384https://onlinelibrary.wiley.com/doi/abs/10.1029/2022EF003384https://agupubs.onlinelibrary.wiley.com/doi/10.1029/2022EF003384>.
- [19] Robert Emberson, Dalia Kirschbaum, and Thomas Stanley. New global characterisation of landslide exposure. *Natural Hazards and Earth System Sciences*, 20(12):3413–3424, 12 2020. ISSN 16849981. doi: 10.5194/NHESS-20-3413-2020.
- [20] Stefano Luigi Gariano and Fausto Guzzetti. Landslides in a changing climate. *Earth-Science Reviews*, 162:227–252, 11 2016. ISSN 0012-8252. doi: 10.1016/J.

EARSCIREV.2016.08.011. URL <https://www.sciencedirect.com/science/article/pii/S0012825216302458#section-cited-by>.

- [21] Hayley J. Fowler, Geert Lenderink, Andreas F. Prein, Seth Westra, Richard P. Allan, Nikolina Ban, Renaud Barbero, Peter Berg, Stephen Blenkinsop, Hong X. Do, Selma Guerreiro, Jan O. Haerter, Elizabeth J. Kendon, Elizabeth Lewis, Christoph Schaer, Ashish Sharma, Gabriele Villarini, Conrad Wasko, and Xuebin Zhang. Anthropogenic intensification of short-duration rainfall extremes. *Nature Reviews Earth & Environment* 2021 2:2, 2(2):107–122, 1 2021. ISSN 2662-138X. doi: 10.1038/s43017-020-00128-6. URL <https://www.nature.com/articles/s43017-020-00128-6>.
- [22] Katherine Calvin, Dipak Dasgupta, Gerhard Krinner, Aditi Mukherji, Peter W. Thorne, Christopher Trisos, José Romero, Paulina Aldunce, Ko Barrett, Gabriel Blanco, William W.L. Cheung, Sarah Connors, Fatima Denton, Aïda Diongue-Niang, David Dodman, Matthias Garschagen, Oliver Geden, Bronwyn Hayward, Christopher Jones, Frank Jotzo, Thelma Krug, Rodel Lasco, Yune-Yi Lee, Valérie Masson-Delmotte, Malte Meinshausen, Katja Mintenbeck, Abdalah Mokssit, Friederike E.L. Otto, Minal Pathak, Anna Pirani, Elvira Poloczanska, Hans-Otto Pörtner, Aromar Revi, Debra C. Roberts, Joyashree Roy, Alex C. Ruane, Jim Skea, Priyadarshi R. Shukla, Raphael Slade, Aimée Slangen, Youba Sokona, Anna A. Sörensson, Melinda Tignor, Detlef van Vuuren, Yi-Ming Wei, Harald Winkler, Panmao Zhai, Zinta Zommers, Jean-Charles Hourcade, Francis X. Johnson, Shonali Pachauri, Nicholas P. Simpson, Chandni Singh, Adelle Thomas, Edmond Totin, Andrés Alegría, Kyle Armour, Birgit Bednar-Friedl, Kornelis Blok, Guéladio Cissé, Frank Dentener, Siri Eriksen, Erich Fischer, Gregory Garner, Céline Guivarch, Marjolijn Haasnoot, Gerrit Hansen, Mathias Hauser, Ed Hawkins, Tim Hermans, Robert Kopp, Noémie Leprince-Ringuet, Jared Lewis, Debora Ley, Chloé Ludden, Leila Niamir, Zebedee Nicholls, Shreya Some, Sophie Szopa, Blair Trewin, Kaj-Ivar van der Wijst, Gundula Winter, Maximilian Witting, Arlene Birt, and Meeyoung Ha. IPCC, 2023: Climate Change 2023: Synthesis Report. Contribution of Working Groups I, II and III to the Sixth Assessment Report of the Intergovernmental Panel on Climate Change [Core Writing Team, H. Lee and J. Romero (eds.)]. IPCC, Geneva, Switzerland. Technical report, Intergovernmental Panel on Climate Change, 7 2023.
- [23] Yu Duan, Mingtao Ding, Yufeng He, Hao Zheng, Ricardo Delgado-Téllez, Sergey Sokratov, Francisco Dourado, and Sven Fuchs. Global projections of future landslide susceptibility under climate change. *Geoscience Frontiers*, 16(4):102074, 7 2025. ISSN 1674-9871. doi: 10.1016/J.GSF.2025.102074. URL <https://www.sciencedirect.com/science/article/pii/S1674987125000799#b0275>.
- [24] D. Kirschbaum, S. B. Kapnick, T. Stanley, and S. Pascale. Changes in Extreme Precipitation and Landslides Over High Mountain Asia. *Geophysical Research Letters*, 47(4):e2019GL085347, 2 2020. ISSN 1944-8007. doi: 10.1029/2019GL085347. URL [/doi/pdf/10.1029/2019GL085347https://onlinelibrary.wiley.com/doi/abs/10.1029/2019GL085347https://agupubs.onlinelibrary.wiley.com/doi/10.1029/2019GL085347](https://doi/pdf/10.1029/2019GL085347https://onlinelibrary.wiley.com/doi/abs/10.1029/2019GL085347https://agupubs.onlinelibrary.wiley.com/doi/10.1029/2019GL085347).
- [25] Qigen Lin, Stefan Steger, Massimiliano Pittore, Jiahui Zhang, Leibin Wang, Tong Jiang, and Ying Wang. Evaluation of potential changes in landslide susceptibility and landslide occurrence frequency in China under climate change. *Science of The Total Environment*, 850:158049, 12 2022. ISSN 0048-9697. doi: 10.1016/J.SCITOTENV.2022.158049. URL https://www.sciencedirect.com/science/article/pii/S0048969722051488?pes=vor&utm_source=iopp&getft_integrator=iopp#f0025.

- [26] Elisa Bozzolan, Elizabeth A Holcombe, Francesca Pianosi, Ivan Marchesini, Massimiliano Alvioli, and Thorsten Wagener. A mechanistic approach to include climate change and unplanned urban sprawl in landslide susceptibility maps. *Science of the total environment*, 858:159412, 2023.
- [27] Kashif Ullah, Yi Wang, Penglei Li, Zhice Fang, Mahfuzur Rahaman, Safi Ullah, and Mohammed Magdy Hamed. Spatiotemporal dynamics of landslide susceptibility under future climate change and land use scenarios. *Environmental Research Letters*, 19(12):124016, 11 2024. ISSN 1748-9326. doi: 10.1088/1748-9326/AD8A72. URL <https://iopscience.iop.org/article/10.1088/1748-9326/ad8a72https://iopscience.iop.org/article/10.1088/1748-9326/ad8a72/meta>.
- [28] Arthur Depicker, Liesbet Jacobs, Nicholus Mboga, Benot Smets, Anton Van Rompaey, Moritz Lennert, Eléonore Wolff, François Kervyn, Caroline Michellier, Olivier Dewitte, and Gerard Govers. Historical dynamics of landslide risk from population and forest-cover changes in the Kivu Rift. *Nature Sustainability* 2021 4:11, 4(11):965–974, 8 2021. ISSN 2398-9629. doi: 10.1038/s41893-021-00757-9. URL <https://www.nature.com/articles/s41893-021-00757-9>.
- [29] Elisa Bozzolan, Elizabeth Holcombe, Francesca Pianosi, and Thorsten Wagener. Including informal housing in slope stability analysis—an application to a data-scarce location in the humid tropics. *Natural Hazards and Earth System Sciences*, 20(11):3161–3177, 2020.
- [30] Ugur Ozturk, Elisa Bozzolan, Elizabeth A. Holcombe, Roopam Shukla, Francesca Pianosi, and Thorsten Wagener. How climate change and unplanned urban sprawl bring more landslides. *Nature* 2022 608:7922, 608(7922):262–265, 8 2022. ISSN 14764687. doi: 10.1038/d41586-022-02141-9. URL <https://www.nature.com/articles/d41586-022-02141-9>.
- [31] Susan L. Cutter, Bryan J. Boruff, and W. Lynn Shirley. Social Vulnerability to Environmental Hazards*. *Social Science Quarterly*, 84(2):242–261, 6 2003. ISSN 1540-6237. doi: 10.1111/1540-6237.8402002. URL </doi/pdf/10.1111/1540-6237.8402002https://onlinelibrary.wiley.com/doi/abs/10.1111/1540-6237.8402002https://onlinelibrary.wiley.com/doi/10.1111/1540-6237.8402002>.
- [32] Bernhard Lehner and Günther Grill. Global river hydrography and network routing: Baseline data and new approaches to study the world’s large river systems. *Hydrological Processes*, 27(15):2171–2186, 7 2013. ISSN 08856087. doi: 10.1002/HYP.9740; REQUESTEDJOURNAL:JOURNAL:10991085;WGROU:STRING:PUBLICATION. URL </doi/pdf/10.1002/hyp.9740https://onlinelibrary.wiley.com/doi/abs/10.1002/hyp.9740https://onlinelibrary.wiley.com/doi/10.1002/hyp.9740>.
- [33] Thomas Stanley and Dalia B Kirschbaum. A heuristic approach to global landslide susceptibility mapping. *Natural hazards*, 87(1):145–164, 2017.
- [34] Laura D Triplett, Morena N Hammer, Stephen B DeLong, Karen B Gran, Carrie E Jennings, Zachary T Engle, Julie K Bartley, Dylan J Blumentritt, Andy J Breckenridge, Stephanie Day, et al. Factors influencing landslide occurrence in low-relief formerly glaciated landscapes: landslide inventory and susceptibility analysis in minnesota, usa. *Natural Hazards*, 121(10):11799–11827, 2025.
- [35] Schiavina M., Freire S., Carioli A., and MacManus K. GHS-POP R2023A - GHS population grid multitemporal (1975-2030), 2023.
- [36] Schiavina M., Melchiorri M., and Pesaresi M. GHS-SMOD R2023A - GHS settlement layers, application of the Degree of Urbanisation methodology (stage I) to GHS-POP R2023A and GHS-BUILT-S R2023A, multitemporal (1975-2030), 2023.

- [37] IPCC. Ippc-national greenhouse gas inventories (tfi), 2019. URL <https://www.ipcc-nggip.iges.or.jp/public/2019rf/corrigenda1.html>.
- [38] Sara Nieto, Edier Aristizábal, and Ugur Ozturk. Coupled evolution of a city and landslides. *Environmental Research Letters*, 20(5):054001, 4 2025. ISSN 1748-9326. doi: 10.1088/1748-9326/ADC4D8. URL <https://iopscience.iop.org/article/10.1088/1748-9326/adc4d8><https://iopscience.iop.org/article/10.1088/1748-9326/adc4d8/meta>.
- [39] Olivier Dewitte, Antoine Dille, Arthur Depicker, Désiré Kubwimana, Jean Claude Maki Mateso, Toussaint Mugaruka Bibentyo, Judith Uwihirwe, and Elise Monsieurs. Constraining landslide timing in a data-scarce context: from recent to very old processes in the tropical environment of the North Tanganyika-Kivu Rift region. *Landslides 2020 18:1*, 18(1):161–177, 7 2020. ISSN 1612-5118. doi: 10.1007/S10346-020-01452-0. URL <https://link.springer.com/article/10.1007/s10346-020-01452-0>.
- [40] Joe Ravetz and Mehebus Sahana. Where is the peri-urban? Mapping the areas ‘around, beyond and between’. *Frontiers in Sustainable Cities*, 7:1436287, 2 2025. ISSN 26249634. doi: 10.3389/FRSC.2025.1436287/BIBTEX.
- [41] Erminia Maricato. The Future of Global Peripheral Cities. *Latin American Perspectives*, 44(2):18–37, 3 2017. ISSN 1552678X. doi: 10.1177/0094582X16685174. URL </doi/pdf/10.1177/0094582X16685174?download=true>.
- [42] S A Sepúlveda and D N Petley. Regional trends and controlling factors of fatal landslides in Latin America and the Caribbean. *Hazards Earth Syst. Sci*, 15:1821–1833, 2015. doi: 10.5194/nhess-15-1821-2015. URL <http://geonames.nga>.
- [43] Allan Lavell, Angel Chávez Eslava, Cinthya Barros Salas, and Diego Miranda Sandoval. Inequality and the social construction of urban disaster risk in multi-hazard contexts: the case of Lima, Peru and the COVID-19 pandemic. *Environment and Urbanization*, 35(1):131–155, 4 2023. ISSN 17460301. doi: 10.1177/09562478221149883;WEBSITE:WEBSITE:SAGE;WGROUPE:STRING:PUBLICATION. URL <https://journals.sagepub.com/doi/10.1177/09562478221149883>.
- [44] Cassiano Bastos Moroz and Annegret H. Thielen. Urban growth and spatial segregation increase disaster risk: lessons learned from the 2023 disaster on the North Coast of São Paulo, Brazil. *Natural Hazards and Earth System Sciences*, 24(9):3299–3314, 9 2024. ISSN 1684-9981. doi: 10.5194/NHESS-24-3299-2024. URL <https://nhess.copernicus.org/articles/24/3299/2024/>.
- [45] Jean Nsabimana, Sabine Henry, Aloys Ndayisenga, Désiré Kubwimana, Olivier Dewitte, François Kervyn, Caroline Michellier, Jean Nsabimana, Sabine Henry, Aloys Ndayisenga, Désiré Kubwimana, Olivier Dewitte, François Kervyn, and Caroline Michellier. Geo-Hydrological Hazard Impacts, Vulnerability and Perception in Bujumbura (Burundi): A High-Resolution Field-Based Assessment in a Sprawling City. *Land 2023, Vol. 12.*, 12(10), 10 2023. ISSN 2073-445X. doi: 10.3390/LAND12101876. URL <https://www.mdpi.com/2073-445X/12/10/1876>.
- [46] Melanie Gall, Kevin A Borden, and Susan L Cutter. When do losses count? six fallacies of natural hazards loss data. *Bulletin of the American Meteorological Society*, 90(6):799–810, 2009.
- [47] Paola Reichenbach, Mauro Rossi, Bruce D. Malamud, Monika Mihir, and Fausto Guzzetti. A review of statistically-based landslide susceptibility models. *Earth-Science Reviews*, 180:

- 60–91, 5 2018. ISSN 0012-8252. doi: 10.1016/J.EARSCIREV.2018.03.001. URL <https://www.sciencedirect.com/science/article/pii/S0012825217305652>.
- [48] Yilin Zhu, Shuangyun Peng, Zhiqiang Lin, Bangmei Huang, Ting Li, Rui Zhang, and Rong Jin. Landslide susceptibility assessment and attribution analysis in yunnan province based on weighted information value-logistic regression model. *Geomatics, Natural Hazards and Risk*, 16(1):2525428, 2025.
- [49] Md Sharafat Chowdhury, Md Naimur Rahman, Md Sujon Sheikh, Md Abu Sayeid, Khan-dakar Hasan Mahmud, and Bibi Hafsa. Gis-based landslide susceptibility mapping using logistic regression, random forest and decision and regression tree models in chattogram district, bangladesh. *Heliyon*, 10(1), 2024.
- [50] Sajid Ali, Peter Biermanns, Rashid Haider, and Klaus Reicherter. Landslide susceptibility mapping by using a geographic information system (gis) along the china–pakistan economic corridor (karakoram highway), pakistan. *Natural Hazards and Earth System Sciences*, 19(5):999–1022, 2019.
- [51] Elisa Bozzolan, Elizabeth Holcombe, Francesca Pianosi, and Thorsten Wagener. Synthetic libraries of urban landslide simulations to identify slope failure hotspots and drivers across spatial scales and landscapes. *Landslides*, 22(3):637–654, 2025.
- [52] Solomon M. Hsiang, Kyle C. Meng, and Mark A. Cane. Civil conflicts are associated with the global climate. *Nature* 2011 476:7361, 476(7361):438–441, 8 2011. ISSN 1476-4687. doi: 10.1038/nature10311. URL <https://www.nature.com/articles/nature10311>.
- [53] Camilo Mora, Daniele Spirandelli, Erik C. Franklin, John Lynham, Michael B. Kantar, Wendy Miles, Charlotte Z. Smith, Kelle Freel, Jade Moy, Leo V. Louis, Evan W. Barba, Keith Bettinger, Abby G. Frazier, John F. Colburn IX, Naota Hanasaki, Ed Hawkins, Yukiko Hirabayashi, Wolfgang Knorr, Christopher M. Little, Kerry Emanuel, Justin Sheffield, Jonathan A. Patz, and Cynthia L. Hunter. Broad threat to humanity from cumulative climate hazards intensified by greenhouse gas emissions. *Nature Climate Change* 2018 8:12, 8(12):1062–1071, 11 2018. ISSN 1758-6798. doi: 10.1038/s41558-018-0315-6. URL <https://www.nature.com/articles/s41558-018-0315-6>.
- [54] James M. Thornton, Mark A. Snethlage, Roger Sayre, Davnah R. Urbach, Daniel Viviroli, Daniele Ehrlich, Veruska Muccione, Philippus Wester, Gregory Insarov, and Carolina Adler. Human populations in the world’s mountains: Spatio-temporal patterns and potential controls. *PLOS ONE*, 17(7):e0271466, 7 2022. ISSN 1932-6203. doi: 10.1371/JOURNAL.PONE.0271466. URL <https://journals.plos.org/plosone/article?id=10.1371/journal.pone.0271466>.
- [55] Arthur Depicker, Gerard Govers, Liesbet Jacobs, Matthias Vanmaercke, Judith Uwhirwe, Benjamin Campforts, Désiré Kubwimana, Jean Claude Mateso, Toussaint Mugaruka Bibentyo, Louis Nahimana, Benoît Smets, and Olivier Dewitte. Mobilization rates of landslides in a changing tropical environment: 60-year record over a large region of the East African Rift. *Geomorphology*, 454:109156, 6 2024. ISSN 0169-555X. doi: 10.1016/J.GEOMORPH.2024.109156. URL <https://www.sciencedirect.com/science/article/pii/S0169555X24001065?via%3Dihub>.
- [56] Antoine Dille, Olivier Dewitte, Alexander L. Handwerker, Nicolas d’Oreye, Dominique Derauw, Gloire Ganza Bamulezi, Guy Ilombe Mawe, Caroline Michellier, Jan Moeyersons, Elise Monsieurs, Toussaint Mugaruka Bibentyo, Sergey Samsonov, Benoît Smets, Matthieu Kervyn, and François Kervyn. Acceleration of a large deep-seated tropical landslide due to urbanization feedbacks. *Nature Geoscience* 2023 15:12, 15(12):1048–1055, 12 2022. ISSN

- 1752-0908. doi: 10.1038/s41561-022-01073-3. URL <https://www.nature.com/articles/s41561-022-01073-3>.
- [57] Bekele Abebe, Francesco Dramis, Giandomenico Fubelli, Mohammed Umer, and Asfawossen Asrat. Landslides in the Ethiopian highlands and the Rift margins. *Journal of African Earth Sciences*, 56(4-5):131–138, 3 2010. ISSN 1464-343X. doi: 10.1016/J.JAFREARSCI.2009.06.006. URL <https://www.sciencedirect.com/science/article/pii/S1464343X09001113?via%3Dihub>.
- [58] EEA. Report on the Ethiopian Economy: Economic Performance and Governance in Ethiopia. Technical report, Ethiopian Economics Association, 5 2025. URL <https://eea-et.org/publication/report-on-the-ethiopian-economy-2025-economic-performance-and-governance-in-ethiopia/>.
- [59] GCR. Ethiopia in Crisis: Deadly Landslides and the Growing Climate Threat, 2025. URL <https://globalclimaterisks.org/insights/blog/ethiopia-in-crisis-deadly-landslides-and-the-growing-climate-threat/>.
- [60] IDMC. Yemen — IDMC - Internal Displacement Monitoring Centre, 2025. URL <https://www.internal-displacement.org/countries/yemen/>.
- [61] IOM. Report on Migration, Environment and Climate Change in Yemen. Technical report, International Organization for Migration (IOM), UN Migration, 2023.
- [62] Jack Rusk, Amina Maharjan, Prakash Tiwari, Tzu Hsin Karen Chen, Sara Shneiderman, Mark Turin, and Karen C. Seto. Multi-hazard susceptibility and exposure assessment of the Hindu Kush Himalaya. *Science of The Total Environment*, 804:150039, 1 2022. ISSN 0048-9697. doi: 10.1016/J.SCITOTENV.2021.150039. URL <https://www.sciencedirect.com/science/article/pii/S0048969721051147#bb0100>.
- [63] Thomas Ruttig. Slippery Slopes: Ecological, social and developmental aspects of the Badakhshan landslide disaster, 5 2014. URL <https://www.afghanistan-analysts.org/en/reports/economy-development-environment/slippery-slopes-ecological-social-and-developmental-aspects-of-the-badakhshan-landslide>
- [64] Hamida Salehzada, Masouda Qasimi, and Shakila Rezayi. Landslide in Badakhshan, Afghanistan, 5 2014. URL https://www.adpc.net/igo/contents/iPrepare/iprepare-news_id.asp?ipid=250.
- [65] Alexandra Witze. Afghan landslide was 'an accident waiting to happen'. *Nature* 2014, 5 2014. ISSN 1476-4687. doi: 10.1038/nature.2014.15158. URL <https://www.nature.com/articles/nature.2014.15158>.
- [66] Bin Tong, Yixiang Zhang, Gan Qi, Jusong Shi, Yuanqiang Wan, Jianyin He, and Xudong Yang. The corresponding countermeasures of landslide risk control under influence of climate change in China. *Geomatics, Natural Hazards and Risk*, 15(1), 12 2024. ISSN 19475713. doi: 10.1080/19475705.2024.2421387;WGROU:STRING:PUBLICATION. URL <https://www.tandfonline.com/doi/pdf/10.1080/19475705.2024.2421387>.
- [67] GFDRR. Learning from Experience Insights from China's Progress in Disaster Risk Management Learning from Experience. Technical report, The World Bank, 2020. URL www.worldbank.org.
- [68] Lei Zhou, Xianhua Wu, Zhonghui Ji, and Ge Gao. Characteristic analysis of rainstorm-induced catastrophe and the countermeasures of flood hazard mitigation about Shenzhen city. *Geomatics, Natural Hazards and Risk*, 8(2):1886–1897, 12 2017. ISSN 19475713.

- doi: 10.1080/19475705.2017.1392368;WGROUP:STRING:PUBLICATION. URL <https://www.tandfonline.com/doi/pdf/10.1080/19475705.2017.1392368>.
- [69] Ilan Kelman. Linking disaster risk reduction, climate change, and the sustainable development goals. *Disaster Prevention and Management*, 26(3):254–258, 6 2017. ISSN 0965-3562. doi: 10.1108/DPM-02-2017-0043. URL <https://dx.doi.org/10.1108/DPM-02-2017-0043>.
- [70] Meg Parsons, Johanna Nalau, Veruska Muccione, Maarten van Aalst, Suraje Dessai, Tess Doeffinger, Xinyu Fu, Toshihiro Hasegawa, Danial Khojasteh, Rahwa Kidane, Benjamin L. Preston, Nicholas P. Simpson, Anita Wreford, and Katharine J. Mach. Critical science for the next decade of climate risk management. *Climate Risk Management*, page 100770, 11 2025. ISSN 2212-0963. doi: 10.1016/J.CRM.2025.100770. URL <https://linkinghub.elsevier.com/retrieve/pii/S2212096325000841>.
- [71] Ian Harris, Timothy J Osborn, Phil Jones, and David Lister. Version 4 of the cru ts monthly high-resolution gridded multivariate climate dataset. *Scientific data*, 7(1):109, 2020.
- [72] Neil James Fantom and Umar Serajuddin. The World Bank’s classification of countries by income. *Policy Research Working Paper Series*, 1 2016. URL <https://ourworldindata.org/grapher/world-bank-income-groups>.
- [73] World bank, worldwide governance indicators, 2024. URL <https://www.worldbank.org/en/publication/worldwide-governance-indicators>.
- [74] Giuseppe Amatulli, Daniel McInerney, Tushar Sethi, Peter Strobl, and Sami Domisch. Geomorpho90m, empirical evaluation and accuracy assessment of global high-resolution geomorphometric layers. *Scientific Data 2020 7:1*, 7(1):162–, 5 2020. ISSN 2052-4463. doi: 10.1038/s41597-020-0479-6. URL <https://www.nature.com/articles/s41597-020-0479-6>.
- [75] Dai Yamazaki, Daiki Ikeshima, Jeffrey C Neal, Fiachra O’Loughlin, Christopher Charles Sampson, Shinjiro Kanae, and Paul D Bates. Merit dem: A new high-accuracy global digital elevation model and its merit to global hydrodynamic modeling. In *AGU fall meeting abstracts*, volume 2017, pages H12C–04, 2017.

Supplementary Information

S1. Average steep area-share by settlement classes (1975 and 2025)

High steep-area shares occur in peri-urban, semi-dense urban classes, particularly in Africa, Asia, and Latin America. Although the share of population in global urban centres grew sharply from 32% to 45% (+2.4 billion people), their steep-area shares remain low across regions.

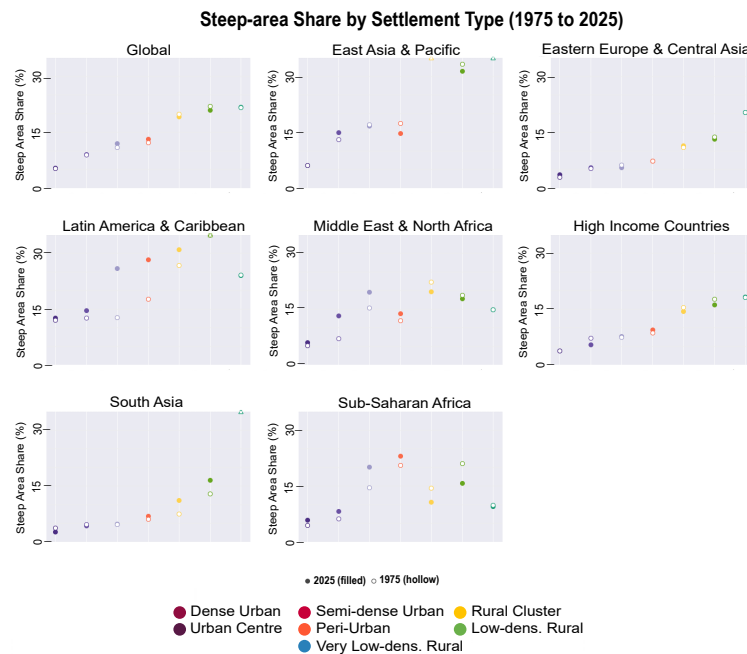


Figure 1: Steep area share by settlement class

S2. Steep-slope population growth vs. non-steep population growth

148 of the 5,393 analysed catchments (about 3%) show population growth on steep slopes exceeding growth on non-steep terrain. These catchments cluster in mountainous regions and represent population growth pressure where flat, buildable land is limited.

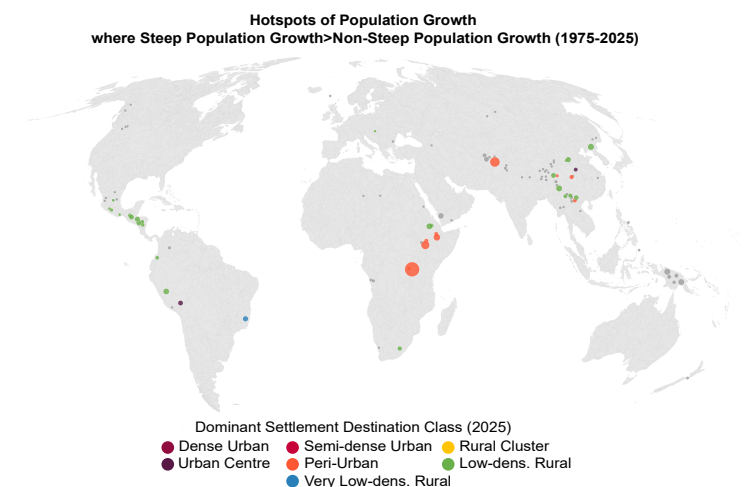


Figure 2: Hotspot catchments of population increase, where absolute growth in steep areas (slope $\geq 10^\circ$) is greater than that in non-steep areas

S3. Steep-terrain population share: 5-year stepwise transitions

Change in population distribution by settlement class in steep areas (with $\geq 10^\circ$ slope), 1975–2025. Most regions show increasing shares in peri-urban and urban classes over time, with notable rural-to-urban transitions in Middle East, North Africa, Sub-Saharan Africa and South Asia (legend same as above)

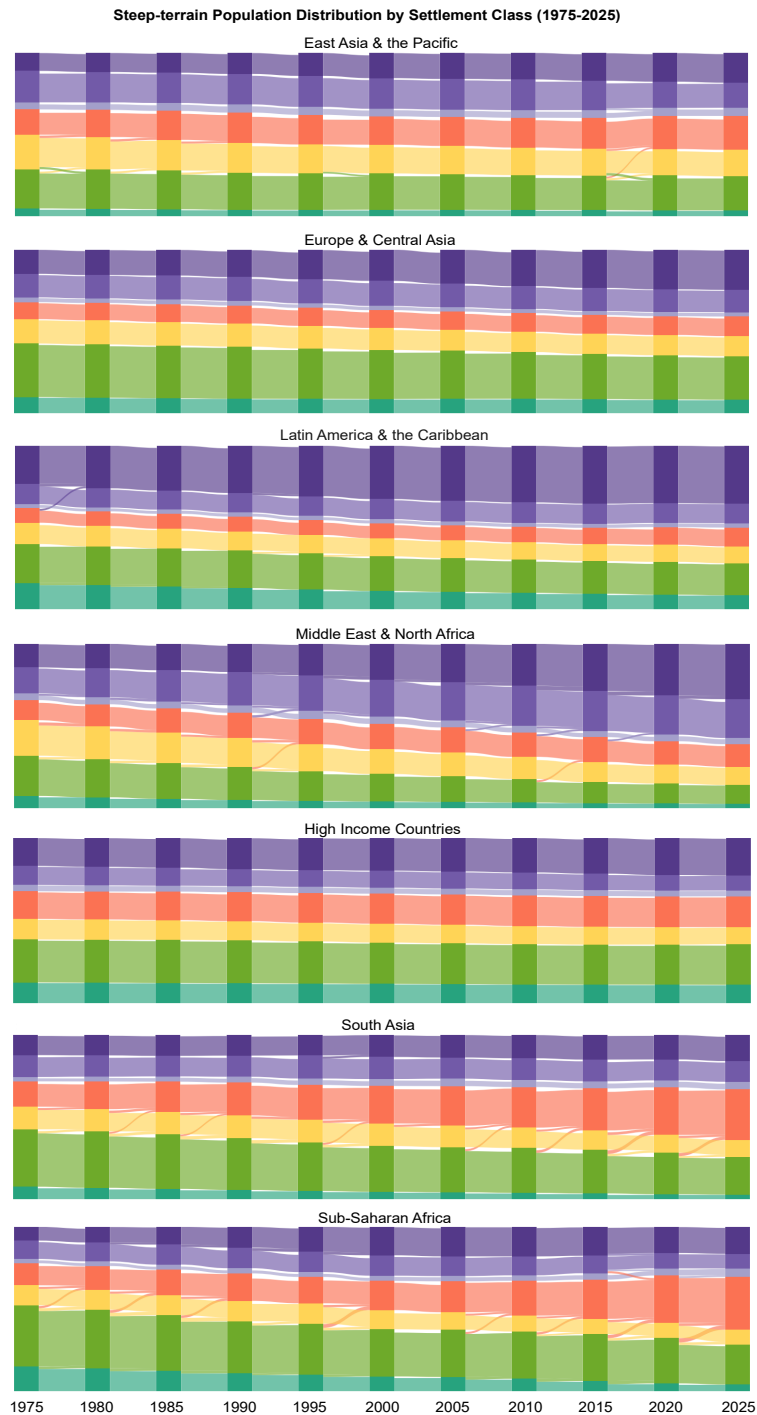


Figure 3: Step-wise population share change on steep terrain as per settlement transitions from 1975 to 2025.

S4. Political stability and steep-slope population growth

Catchments with the highest steep-slope population growth lie in countries ranking consistently low in the UN-defined ‘Political Stability and Absence of Violence’ index. The index reflects perceptions of the likelihood of political instability and politically motivated violence, including terrorism, and is reported as a national rank from 1 to 100, where 1 indicates the lowest stability and 100 the highest.

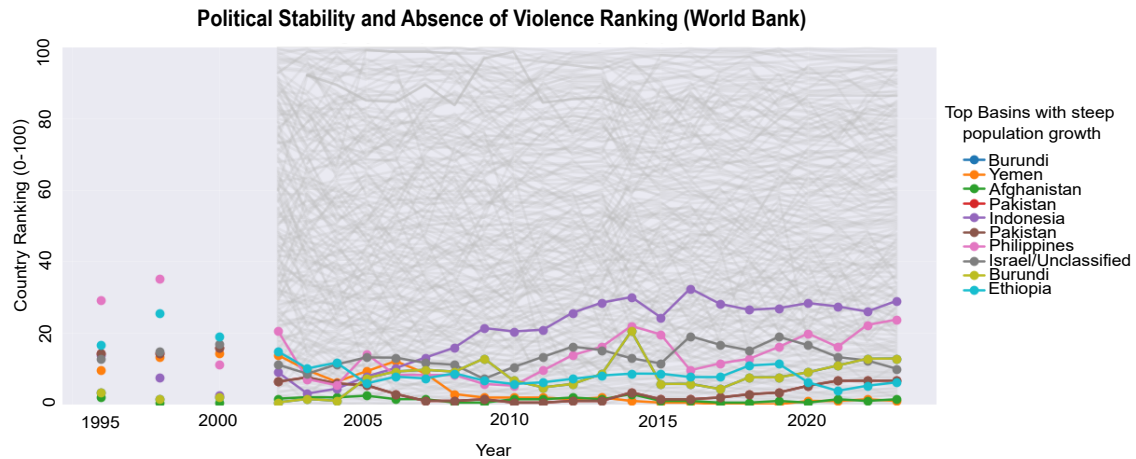


Figure 4: World Bank Political Stability and Absence of Violence Rankings

S5. Definitions and contextual indicators (map annotations)

We label selected hotspot regions using four recurring contextual factors: rapid urbanisation, informal settlements, low institutional capacity, and political instability. These labels are used to support interpretation of patterns in the maps and are not used as quantitative predictors in the analysis.

Definitions follow established usage in the literature:

0.0.1 Rapid urbanisation

Fast growth of the urban population and/or urban extent, often accompanied by unplanned or poorly coordinated expansion when infrastructure and planning do not keep pace [1].

0.0.2 Informal settlements

Residential areas where (i) residents often lack secure tenure, (ii) areas are underserved by basic services and infrastructure, and (iii) housing may not comply with planning and building regulations, with settlements often located in hazard-prone or environmentally marginal land [2].

0.0.3 Low institutional capacity

Institutional (or governance) capacity can be defined as the ability of governance institutions and actors to plan, coordinate, finance, implement, evaluate, and adjust policies and measures over time, including under uncertainty and rapid change [3].

0.0.4 Political instability

For our analysis, political instability is operationalized using the World Bank WGI Political Stability and Absence of Violence/Terrorism indicator, which measures perceptions of the likelihood of political instability and/or politically motivated violence, including terrorism (reported as an estimate and percentile ranks) [4].

S6. Detailed examples of regions with growing slope-instability exposure facing multiple challenges

Population exposure on steep terrain emerges where physical constraints intersect with settlement expansion, weak institutional capacity, or both (Figure 4 in the main text). These constraints can include steep topography, triggering factors or multi-hazard environments. Lack of institutional capacity can result from economic and political instability, weak regulation or absence of research. Settlement expansion in the form of rapid urbanization or informal construction, with displacement adding further pressure. Slope exposure reflects constrained choices under climate, conflict, and land pressure.

- The African Rift Valley lakes are dotted with densely populated cities like Bukavu in the Democratic Republic of the Congo (DRC) and Bujumbura, the largest city in Burundi. These cities have experienced rapid, often unplanned expansion. There is also evidence of anthropogenic acceleration of deep-seated landslides in the region due to urbanisation [5, 6]. In the backdrop of conflict and political instability, cities are often seen as safe havens. Here, basic necessities such as safety and access to food and water take precedence over slope-related hazard avoidance [7]. The vulnerability of people is heightened by the presence of other hazards further, such as flash floods [8]. This combination of multi-hazards and lack of capacity is not sustainable, especially in the face of projected climate-related extremes in the region [9].

- The Ethiopian Highlands region is also identified in our study as a hotspot. Here, steep relief coincides with rapid population growth and limited availability of flat land. Landslides in this region are primarily triggered by intense and recurrent summer rainfall [10]. These events cause repeated loss of life, damage to infrastructure, and impacts on agricultural land and livelihoods [11]. In July 2024, Ethiopia experienced its deadliest recorded landslide, with more than 230 fatalities and over 15,000 people displaced during prolonged rainfall [12]. Climate stress is making rainfall events erratic, impacting not only landslides, but also affecting food security, migration patterns and health [13]. Higher elevations are known to act as “refugia” against extreme heat in the region [14]. Additionally, Ethiopia’s economy is highly dependent on agriculture, which supports around 65% of the population and is increasingly affected by droughts, floods, land degradation, and declining yields [15, 16]. At the same time, climate-sensitive health risks, such as malaria, heat stress, and waterborne diseases further strain households and health systems, particularly among vulnerable groups [17]. Thus, settlement decisions are shaped by access to land, livelihoods, and basic services under constrained conditions. Steep-slope exposure in Ethiopia reflects the accumulation of climatic stress, livelihood pressure, and limited adaptive capacity, rather than an active choice to occupy hazardous terrain.

- The southern part of Yemen, also identified as a steep-population increase hotspot, is another region where steep terrain, conflict, and environmental stress intersect. Yemen’s mountainous topography and highly variable rainfall make it prone to rainfall-triggered landslides, particularly where informal housing occupies marginal slopes and unstable soils [18, 19]. Climate-driven increases in intense rainfall and flash flooding have repeatedly damaged housing and infrastructure, accelerating displacement and secondary migration [20]. Ongoing conflict has weakened land governance, emergency coordination, and hazard monitoring, while forcing more than four million internally displaced people to settle in hazard-prone urban and peri-urban areas with limited services [21, 22]. In this context as well, steep-slope exposure reflects constrained choices under displacement, insecurity, and environmental degradation.

- Paralleling our analyses, the Hindu Kush Mountains in Afghanistan and Northern Pakistan have also been identified in literature as a hotspot for overlapping geophysical and hydrological hazards [23, 24]. In this mountainous region, where population growth rates are some of the highest and flat, arable land is limited, people in rural areas are often forced to live on steep slopes [25]. Moreover, a lack of monitoring infrastructure and limited response capacity make this region more vulnerable to hazards. This limitation was highlighted during a deadly landslide in Badakhshan region in 2014. Dubbed by experts as an ‘accident waiting to happen’ [26], authorities, drained by decades-long conflicts, not only failed to mitigate the event but also lacked rescue capacity. The death toll post-disaster was reported with such a lack of precision that it was in the wide range of 350 to more than 2000 people [27]. Regional conflict, slow economic development and political instability, compounded by the existing population pressure and unstable geology, make this region extremely vulnerable.

- China provides a contrasting case where steep-slope exposure is increasing under high development and institutional capacity. Along the eastern coast of China, our analysis identifies clusters of catchments with strong population growth on steep terrain. Recent studies show that climate change is altering hydro-meteorological drivers of landslides, while rapid urbanisation and infrastructure expansion are increasing exposure and the value of assets at risk [28]. Extreme events, such as the July 2020 rainfall in Zhengzhou city, triggered hundreds of landslides in areas previously considered low-susceptible to landslides, illustrating how the hazard is expanding into new regions. Recent studies also suggest a climate-driven increase in landslide probability under future warming [29]. Extreme, short-duration rainstorms in highly urbanised, low-lying and hilly coastal cities like Shenzhen cause compound disasters, including flooding, waterlogging and slope failures, such as during the 2008 floods and landslide event [30]. Such events have large human and economic impacts.

S7. Population-dataset robustness: World-Pop and GHS-Pop comparison

Population-dataset robustness was assessed by repeating the steep-slope growth analysis using WorldPop and comparing results to GHS-POP over the overlap period 2000–2020. In the top 50 catchments, 40 overlapped, with 10 as per WorldPop and 10 according to GHS. In the map comparison (Fig S5), the non-overlapping catchments typically occur in the same broader neighbourhood of overlapping catchments, rather than appearing in completely different parts of the world. The Spearman rank correlation of $\rho = 0.79$ was obtained for catchment-level positive steep-slope growth rank.

Top 50 catchments by steep-slope population growth (2000-2020)

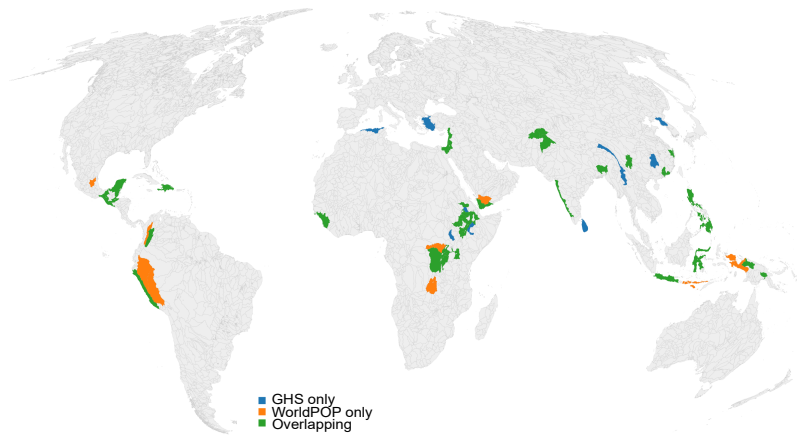


Figure 5: Top 50 steep-slope population growth catchments according to different population datasets

S8. Slope-threshold sensitivity

Slope-threshold sensitivity was assessed by repeating key analyses using alternative slope thresholds (8°, 10°, 12° and 15°) to evaluate how results depend on the definition of ‘steep’. The plot S4 shows how the share of each income group’s population counted as “exposed” changes as the slope threshold is tightened (8°, 10°, 12°, 15°). As expected, the share declines for all groups, but the ranking and separation between groups remain similar, meaning the pattern is not an artefact of one cut-off. We use 10° because it is a widely used benchmark in global landslide studies and is representative of conditions where rainfall-triggered landslides occur frequently [31-33]. It balances capturing meaningful hillslope exposure without restricting the analysis only to the steepest terrain.

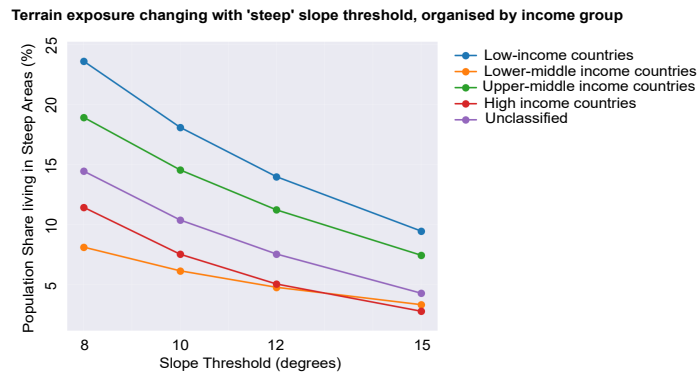


Figure 6: Sensitivity of steep-area population share with varying slope-thresholds

S9. Population living on steep terrain by settlement class, 1975–2025

Tables 1-9 summarise the population living on steep terrain (slope $\geq 10^\circ$) from 1975 to 2025, based on the analysis with GHSL 1km products. Table 1 reports global totals and the percentage of the global population living on steep terrain. The following regional tables report, for each time step, the steep-slope population by settlement class (millions) together with the share of each class within the region’s total steep-slope population.

Table 1: Global population living on steep terrain (slope $\geq 10^\circ$), 1975–2025.

| Year | Total population (billions) | Steep population (millions) | Share on steep terrain (%) |
|------|-----------------------------|-----------------------------|----------------------------|
| 1975 | 4.07 | 493.99 | 12.14 |
| 1980 | 4.44 | 531.34 | 11.96 |
| 1985 | 4.86 | 572.86 | 11.78 |
| 1990 | 5.32 | 618.30 | 11.63 |
| 1995 | 5.74 | 646.33 | 11.25 |
| 2000 | 6.15 | 665.85 | 10.83 |
| 2005 | 6.56 | 694.63 | 10.59 |
| 2010 | 6.99 | 727.30 | 10.41 |
| 2015 | 7.43 | 764.75 | 10.30 |
| 2020 | 7.84 | 804.05 | 10.25 |
| 2025 | 8.19 | 834.74 | 10.19 |

Table 2: East Asia and Pacific: steep-slope population by settlement class, 1975–2025.

| Year | Very low-dens rural | | Low-dens rural | | Rural cluster | | Peri-urban | | Semi-dense urban | | Dense urban | | Urban centre | |
|------|---------------------|-------|----------------|-------|---------------|-------|------------|-------|------------------|-------|-------------|-------|--------------|-------|
| | Pop | Share | Pop | Share | Pop | Share | Pop | Share | Pop | Share | Pop | Share | Pop | Share |
| 1975 | 10.64 | 4.8 | 53.72 | 24.0 | 47.31 | 21.1 | 34.63 | 15.5 | 9.67 | 4.3 | 43.09 | 19.2 | 24.82 | 11.1 |
| 1980 | 10.92 | 4.6 | 57.81 | 24.2 | 47.20 | 19.7 | 39.65 | 16.6 | 10.97 | 4.6 | 44.49 | 18.6 | 28.05 | 11.7 |
| 1985 | 10.90 | 4.3 | 60.70 | 23.7 | 48.08 | 18.8 | 45.38 | 17.7 | 12.40 | 4.8 | 47.43 | 18.5 | 31.25 | 12.2 |
| 1990 | 10.79 | 3.9 | 62.26 | 22.6 | 50.14 | 18.2 | 51.48 | 18.7 | 13.79 | 5.0 | 51.35 | 18.6 | 35.64 | 12.9 |
| 1995 | 10.88 | 3.9 | 62.36 | 22.3 | 49.69 | 17.7 | 50.98 | 18.2 | 13.55 | 4.8 | 53.12 | 19.0 | 39.61 | 14.1 |
| 2000 | 10.96 | 4.0 | 61.35 | 22.2 | 48.52 | 17.6 | 48.04 | 17.4 | 12.69 | 4.6 | 51.77 | 18.7 | 42.87 | 15.5 |
| 2005 | 11.06 | 3.9 | 61.54 | 21.8 | 48.57 | 17.2 | 49.98 | 17.7 | 12.72 | 4.5 | 52.86 | 18.8 | 45.15 | 16.0 |
| 2010 | 11.05 | 3.8 | 61.82 | 21.3 | 49.01 | 16.9 | 52.86 | 18.2 | 13.49 | 4.6 | 54.55 | 18.8 | 47.29 | 16.3 |
| 2015 | 11.17 | 3.7 | 63.20 | 21.1 | 49.28 | 16.5 | 56.18 | 18.8 | 14.16 | 4.7 | 53.76 | 18.0 | 51.11 | 17.1 |
| 2020 | 10.87 | 3.6 | 65.36 | 21.4 | 49.58 | 16.2 | 61.90 | 20.2 | 14.94 | 4.9 | 49.11 | 16.1 | 54.10 | 17.7 |
| 2025 | 10.85 | 3.5 | 64.07 | 20.9 | 49.93 | 16.3 | 63.61 | 20.7 | 15.39 | 5.0 | 47.11 | 15.3 | 56.21 | 18.3 |

Table 3: Europe and Central Asia: steep-slope population by settlement class, 1975–2025.

| Year | Very low-dens rural | | Low-dens rural | | Rural cluster | | Peri-urban | | Semi-dense urban | | Dense urban | | Urban centre | |
|------|---------------------|-------|----------------|-------|---------------|-------|------------|-------|------------------|-------|-------------|-------|--------------|-------|
| | Pop | Share | Pop | Share | Pop | Share | Pop | Share | Pop | Share | Pop | Share | Pop | Share |
| 1975 | 2.92 | 9.9 | 9.69 | 32.8 | 4.42 | 14.9 | 3.08 | 10.4 | 0.86 | 2.9 | 4.27 | 14.4 | 4.35 | 14.7 |
| 1980 | 2.95 | 9.5 | 10.15 | 32.6 | 4.59 | 14.7 | 3.31 | 10.6 | 0.87 | 2.8 | 4.46 | 14.3 | 4.81 | 15.4 |
| 1985 | 2.98 | 9.1 | 10.53 | 32.3 | 4.72 | 14.5 | 3.56 | 10.9 | 0.90 | 2.8 | 4.80 | 14.7 | 5.15 | 15.8 |
| 1990 | 3.00 | 8.8 | 10.82 | 31.9 | 4.81 | 14.2 | 3.72 | 11.0 | 0.99 | 2.9 | 4.92 | 14.5 | 5.66 | 16.7 |
| 1995 | 2.98 | 8.8 | 10.46 | 30.8 | 4.70 | 13.9 | 3.73 | 11.0 | 0.94 | 2.8 | 5.00 | 14.7 | 6.13 | 18.1 |
| 2000 | 2.94 | 8.7 | 10.20 | 30.0 | 4.58 | 13.5 | 3.69 | 10.9 | 0.87 | 2.6 | 5.21 | 15.3 | 6.47 | 19.0 |
| 2005 | 2.96 | 8.8 | 9.91 | 29.4 | 4.34 | 12.9 | 3.74 | 11.1 | 0.88 | 2.6 | 4.86 | 14.4 | 7.01 | 20.8 |
| 2010 | 2.96 | 8.8 | 9.57 | 28.6 | 4.17 | 12.4 | 3.80 | 11.4 | 0.87 | 2.6 | 4.67 | 13.9 | 7.46 | 22.3 |
| 2015 | 2.96 | 8.6 | 9.44 | 27.5 | 4.28 | 12.5 | 3.91 | 11.4 | 0.86 | 2.5 | 4.85 | 14.1 | 8.01 | 23.3 |
| 2020 | 2.94 | 8.4 | 9.47 | 27.1 | 4.35 | 12.4 | 4.02 | 11.5 | 0.91 | 2.6 | 4.84 | 13.8 | 8.47 | 24.2 |
| 2025 | 2.91 | 8.2 | 9.44 | 26.7 | 4.35 | 12.3 | 4.25 | 12.0 | 0.93 | 2.6 | 4.85 | 13.7 | 8.68 | 24.5 |

Table 4: Global: steep-slope population by settlement class, 1975–2025.

| Year | Very low-dens rural | | Low-dens rural | | Rural cluster | | Peri-urban | | Semi-dense urban | | Dense urban | | Urban centre | |
|------|---------------------|-------|----------------|-------|---------------|-------|------------|-------|------------------|-------|-------------|-------|--------------|-------|
| | Pop | Share | Pop | Share | Pop | Share | Pop | Share | Pop | Share | Pop | Share | Pop | Share |
| 1975 | 43.30 | 8.8 | 132.94 | 26.9 | 83.95 | 17.0 | 70.32 | 14.2 | 17.65 | 3.6 | 77.42 | 15.7 | 68.40 | 13.8 |
| 1980 | 44.18 | 8.3 | 142.15 | 26.8 | 85.77 | 16.1 | 79.76 | 15.0 | 19.81 | 3.7 | 81.21 | 15.3 | 78.45 | 14.8 |
| 1985 | 44.57 | 7.8 | 150.04 | 26.2 | 89.03 | 15.5 | 91.02 | 15.9 | 22.30 | 3.9 | 87.39 | 15.3 | 88.51 | 15.5 |
| 1990 | 44.67 | 7.2 | 155.76 | 25.2 | 94.08 | 15.2 | 102.69 | 16.6 | 25.04 | 4.0 | 95.09 | 15.4 | 100.97 | 16.3 |
| 1995 | 44.84 | 6.9 | 158.21 | 24.5 | 95.99 | 14.9 | 106.17 | 16.4 | 25.78 | 4.0 | 100.98 | 15.6 | 114.35 | 17.7 |
| 2000 | 44.71 | 6.7 | 158.55 | 23.8 | 96.42 | 14.5 | 109.62 | 16.5 | 25.78 | 3.9 | 103.23 | 15.5 | 127.54 | 19.2 |
| 2005 | 45.44 | 6.5 | 163.10 | 23.5 | 96.92 | 14.0 | 117.66 | 16.9 | 26.60 | 3.8 | 106.74 | 15.4 | 138.17 | 19.9 |
| 2010 | 45.18 | 6.2 | 167.81 | 23.1 | 97.93 | 13.5 | 128.05 | 17.6 | 28.04 | 3.9 | 111.69 | 15.4 | 148.60 | 20.4 |
| 2015 | 44.56 | 5.8 | 174.04 | 22.8 | 99.45 | 13.0 | 140.94 | 18.4 | 30.28 | 4.0 | 113.38 | 14.8 | 162.10 | 21.2 |
| 2020 | 43.05 | 5.4 | 181.58 | 22.6 | 101.79 | 12.7 | 163.11 | 20.3 | 32.97 | 4.1 | 109.76 | 13.7 | 171.78 | 21.4 |
| 2025 | 42.51 | 5.1 | 179.96 | 21.6 | 103.67 | 12.4 | 179.29 | 21.5 | 36.01 | 4.3 | 109.90 | 13.2 | 183.40 | 22.0 |

Table 5: Latin America and the Caribbean: steep-slope population by settlement class, 1975–2025.

| Year | Very low-dens rural Pop | Low-dens rural Share | Low-dens rural Pop | Rural cluster Share | Rural cluster Pop | Peri-urban Share | Peri-urban Pop | Semi-dense urban Share | Semi-dense urban Pop | Dense urban Share | Dense urban Pop | Urban centre Share | Urban centre Pop | |
|------|-------------------------|----------------------|--------------------|---------------------|-------------------|------------------|----------------|------------------------|----------------------|-------------------|-----------------|--------------------|------------------|------|
| 1975 | 9.68 | 16.0 | 14.43 | 23.9 | 7.89 | 13.0 | 5.52 | 9.1 | 1.34 | 2.2 | 7.54 | 12.5 | 14.07 | 23.3 |
| 1980 | 9.89 | 14.8 | 15.82 | 23.6 | 8.33 | 12.5 | 6.01 | 9.0 | 1.55 | 2.3 | 7.88 | 11.8 | 17.42 | 26.0 |
| 1985 | 10.15 | 13.8 | 17.25 | 23.5 | 8.82 | 12.0 | 6.74 | 9.2 | 1.87 | 2.5 | 8.62 | 11.7 | 20.12 | 27.4 |
| 1990 | 10.31 | 12.9 | 18.46 | 23.1 | 9.24 | 11.6 | 7.32 | 9.2 | 1.98 | 2.5 | 9.55 | 11.9 | 23.08 | 28.9 |
| 1995 | 10.39 | 12.0 | 19.20 | 22.1 | 9.81 | 11.3 | 7.80 | 9.0 | 2.31 | 2.7 | 10.43 | 12.0 | 26.78 | 30.9 |
| 2000 | 10.35 | 11.1 | 19.72 | 21.2 | 10.38 | 11.2 | 8.40 | 9.0 | 2.39 | 2.6 | 11.46 | 12.3 | 30.34 | 32.6 |
| 2005 | 10.42 | 10.6 | 20.48 | 20.8 | 10.68 | 10.8 | 8.99 | 9.1 | 2.46 | 2.5 | 12.30 | 12.5 | 33.30 | 33.8 |
| 2010 | 10.35 | 10.0 | 20.99 | 20.3 | 10.96 | 10.6 | 9.75 | 9.4 | 2.54 | 2.5 | 12.94 | 12.5 | 35.82 | 34.7 |
| 2015 | 10.26 | 9.5 | 21.64 | 20.0 | 11.33 | 10.5 | 10.71 | 9.9 | 2.70 | 2.5 | 13.29 | 12.3 | 38.39 | 35.4 |
| 2020 | 10.14 | 8.9 | 22.96 | 20.1 | 11.92 | 10.4 | 12.35 | 10.8 | 2.93 | 2.6 | 13.84 | 12.1 | 40.06 | 35.1 |
| 2025 | 10.04 | 8.5 | 23.31 | 19.7 | 12.23 | 10.3 | 13.62 | 11.5 | 3.15 | 2.7 | 14.20 | 12.0 | 42.01 | 35.4 |

Table 6: Middle East and North Africa: steep-slope population by settlement class, 1975–2025.

| Year | Very low-dens rural Pop | Low-dens rural Share | Low-dens rural Pop | Rural cluster Share | Rural cluster Pop | Peri-urban Share | Peri-urban Pop | Semi-dense urban Share | Semi-dense urban Pop | Dense urban Share | Dense urban Pop | Urban centre Share | Urban centre Pop | |
|------|-------------------------|----------------------|--------------------|---------------------|-------------------|------------------|----------------|------------------------|----------------------|-------------------|-----------------|--------------------|------------------|------|
| 1975 | 1.13 | 7.4 | 3.72 | 24.5 | 3.28 | 21.6 | 1.86 | 12.3 | 0.63 | 4.1 | 2.40 | 15.8 | 2.18 | 14.3 |
| 1980 | 1.16 | 6.6 | 4.08 | 23.2 | 3.50 | 19.9 | 2.38 | 13.5 | 0.77 | 4.4 | 3.08 | 17.5 | 2.62 | 14.9 |
| 1985 | 1.18 | 5.7 | 4.50 | 21.8 | 3.82 | 18.5 | 3.02 | 14.6 | 0.87 | 4.2 | 3.93 | 19.1 | 3.31 | 16.0 |
| 1990 | 1.18 | 4.9 | 4.82 | 20.1 | 4.23 | 17.6 | 3.67 | 15.3 | 1.11 | 4.6 | 4.85 | 20.2 | 4.10 | 17.1 |
| 1995 | 1.17 | 4.4 | 4.84 | 18.1 | 4.34 | 16.3 | 4.12 | 15.5 | 1.30 | 4.9 | 5.80 | 21.7 | 5.10 | 19.1 |
| 2000 | 1.17 | 4.1 | 4.84 | 16.7 | 4.35 | 15.1 | 4.47 | 15.5 | 1.29 | 4.5 | 6.49 | 22.5 | 6.30 | 21.8 |
| 2005 | 1.17 | 3.8 | 4.86 | 15.7 | 4.47 | 14.4 | 4.74 | 15.3 | 1.28 | 4.1 | 7.25 | 23.4 | 7.25 | 23.4 |
| 2010 | 1.17 | 3.5 | 4.85 | 14.3 | 4.57 | 13.5 | 5.04 | 14.9 | 1.33 | 3.9 | 8.28 | 24.4 | 8.64 | 25.5 |
| 2015 | 1.16 | 3.1 | 4.89 | 12.9 | 4.66 | 12.2 | 5.74 | 15.1 | 1.41 | 3.7 | 9.28 | 24.4 | 10.91 | 28.7 |
| 2020 | 1.16 | 2.8 | 4.96 | 12.2 | 4.70 | 11.5 | 5.81 | 14.2 | 1.64 | 4.0 | 9.72 | 23.8 | 12.83 | 31.4 |
| 2025 | 1.15 | 2.6 | 5.01 | 11.5 | 4.86 | 11.1 | 6.02 | 13.7 | 1.66 | 3.8 | 10.34 | 23.6 | 14.73 | 33.7 |

Table 7: Other high income countries: steep-slope population by settlement class, 1975–2025.

| Year | Very low-dens rural Pop | Low-dens rural Share | Low-dens rural Pop | Rural cluster Share | Rural cluster Pop | Peri-urban Share | Peri-urban Pop | Semi-dense urban Share | Semi-dense urban Pop | Dense urban Share | Dense urban Pop | Urban centre Share | Urban centre Pop | |
|------|-------------------------|----------------------|--------------------|---------------------|-------------------|------------------|----------------|------------------------|----------------------|-------------------|-----------------|--------------------|------------------|------|
| 1975 | 8.61 | 12.5 | 17.87 | 26.0 | 8.56 | 12.5 | 11.48 | 16.7 | 2.60 | 3.8 | 7.94 | 11.6 | 11.62 | 16.9 |
| 1980 | 8.77 | 12.4 | 18.45 | 26.0 | 8.67 | 12.2 | 11.99 | 16.9 | 2.63 | 3.7 | 7.96 | 11.2 | 12.37 | 17.5 |
| 1985 | 8.87 | 12.2 | 19.04 | 26.1 | 8.72 | 12.0 | 12.57 | 17.3 | 2.59 | 3.6 | 7.98 | 11.0 | 13.08 | 18.0 |
| 1990 | 8.95 | 12.0 | 19.35 | 26.0 | 8.63 | 11.6 | 13.00 | 17.5 | 2.79 | 3.8 | 7.65 | 10.3 | 14.01 | 18.8 |
| 1995 | 8.97 | 11.9 | 19.24 | 25.5 | 8.66 | 11.5 | 13.46 | 17.8 | 2.82 | 3.7 | 7.66 | 10.1 | 14.73 | 19.5 |
| 2000 | 8.95 | 11.7 | 19.20 | 25.0 | 8.76 | 11.4 | 13.93 | 18.2 | 2.80 | 3.6 | 7.91 | 10.3 | 15.17 | 19.8 |
| 2005 | 9.00 | 11.5 | 19.37 | 24.7 | 8.80 | 11.2 | 14.40 | 18.4 | 2.81 | 3.6 | 8.09 | 10.3 | 15.87 | 20.3 |
| 2010 | 9.06 | 11.3 | 19.57 | 24.4 | 8.79 | 11.0 | 14.92 | 18.6 | 2.90 | 3.6 | 8.19 | 10.2 | 16.71 | 20.9 |
| 2015 | 9.06 | 11.2 | 19.63 | 24.2 | 8.69 | 10.7 | 15.11 | 18.7 | 2.91 | 3.6 | 8.08 | 10.0 | 17.51 | 21.6 |
| 2020 | 9.04 | 11.1 | 19.75 | 24.3 | 8.60 | 10.6 | 15.07 | 18.6 | 2.85 | 3.5 | 7.65 | 9.4 | 18.23 | 22.5 |
| 2025 | 8.99 | 11.1 | 20.00 | 24.6 | 8.44 | 10.4 | 15.14 | 18.6 | 2.84 | 3.5 | 7.28 | 9.0 | 18.55 | 22.8 |

Table 8: South Asia: steep-slope population by settlement class, 1975–2025.

| Year | Very low-dens rural Pop | Low-dens rural Share | Low-dens rural Pop | Rural cluster Share | Rural cluster Pop | Peri-urban Share | Peri-urban Pop | Semi-dense urban Share | Semi-dense urban Pop | Dense urban Share | Dense urban Pop | Urban centre Share | Urban centre Pop | |
|------|-------------------------|----------------------|--------------------|---------------------|-------------------|------------------|----------------|------------------------|----------------------|-------------------|-----------------|--------------------|------------------|------|
| 1975 | 3.57 | 7.6 | 16.42 | 34.9 | 6.48 | 13.8 | 7.26 | 15.4 | 1.24 | 2.6 | 6.27 | 13.3 | 5.79 | 12.3 |
| 1980 | 3.54 | 6.9 | 17.56 | 34.3 | 6.92 | 13.5 | 8.63 | 16.9 | 1.49 | 2.9 | 6.62 | 12.9 | 6.39 | 12.5 |
| 1985 | 3.48 | 6.3 | 18.41 | 33.2 | 7.48 | 13.5 | 10.25 | 18.5 | 1.78 | 3.2 | 6.91 | 12.5 | 7.09 | 12.8 |
| 1990 | 3.40 | 5.6 | 19.05 | 31.5 | 8.40 | 13.9 | 12.07 | 20.0 | 2.15 | 3.5 | 7.79 | 12.9 | 7.64 | 12.6 |
| 1995 | 3.31 | 5.0 | 19.69 | 29.5 | 9.37 | 14.0 | 14.05 | 21.0 | 2.61 | 3.9 | 9.39 | 14.1 | 8.35 | 12.5 |
| 2000 | 3.22 | 4.5 | 19.97 | 27.8 | 9.88 | 13.8 | 16.39 | 22.8 | 3.02 | 4.2 | 9.65 | 13.4 | 9.64 | 13.4 |
| 2005 | 3.22 | 4.2 | 21.10 | 27.5 | 9.99 | 13.0 | 18.52 | 24.1 | 3.48 | 4.5 | 9.90 | 12.9 | 10.57 | 13.8 |
| 2010 | 3.11 | 3.9 | 22.06 | 27.3 | 10.02 | 12.4 | 19.98 | 24.7 | 3.46 | 4.3 | 10.68 | 13.2 | 11.53 | 14.3 |
| 2015 | 2.98 | 3.5 | 22.77 | 26.7 | 9.95 | 11.7 | 21.83 | 25.6 | 3.70 | 4.3 | 11.26 | 13.2 | 12.83 | 15.0 |
| 2020 | 2.75 | 3.0 | 23.08 | 25.2 | 9.92 | 10.8 | 26.43 | 28.9 | 3.92 | 4.3 | 11.65 | 12.7 | 13.67 | 15.0 |
| 2025 | 2.70 | 2.8 | 22.36 | 23.0 | 10.02 | 10.3 | 29.86 | 30.7 | 4.51 | 4.6 | 12.23 | 12.6 | 15.52 | 16.0 |

Table 9: Sub-Saharan Africa: steep-slope population by settlement class, 1975–2025.

| Year | Very low-dens Pop | rural Share | Low-dens rural Pop | rural Share | Rural cluster Pop | Share | Peri-urban Pop | Share | Semi-dense urban Pop | Share | Dense urban Pop | Share | Urban centre Pop | Share |
|------|-------------------|-------------|--------------------|-------------|-------------------|-------|----------------|-------|----------------------|-------|-----------------|-------|------------------|-------|
| 1975 | 6.52 | 15.1 | 16.07 | 37.2 | 5.25 | 12.2 | 5.79 | 13.4 | 1.14 | 2.6 | 4.83 | 11.2 | 3.60 | 8.3 |
| 1980 | 6.71 | 13.9 | 17.18 | 35.7 | 5.76 | 12.0 | 7.02 | 14.6 | 1.36 | 2.8 | 5.54 | 11.5 | 4.56 | 9.5 |
| 1985 | 6.78 | 12.4 | 18.44 | 33.8 | 6.55 | 12.0 | 8.58 | 15.7 | 1.68 | 3.1 | 6.63 | 12.2 | 5.88 | 10.8 |
| 1990 | 6.80 | 10.9 | 19.79 | 31.7 | 7.75 | 12.4 | 10.44 | 16.7 | 1.98 | 3.2 | 7.85 | 12.6 | 7.86 | 12.6 |
| 1995 | 6.92 | 10.1 | 21.21 | 31.0 | 8.49 | 12.4 | 10.99 | 16.1 | 2.01 | 2.9 | 8.42 | 12.3 | 10.41 | 15.2 |
| 2000 | 6.88 | 9.0 | 22.04 | 28.7 | 8.97 | 11.7 | 13.60 | 17.7 | 2.47 | 3.2 | 9.52 | 12.4 | 13.27 | 17.3 |
| 2005 | 7.38 | 8.6 | 24.60 | 28.8 | 9.06 | 10.6 | 16.09 | 18.8 | 2.72 | 3.2 | 10.26 | 12.0 | 15.34 | 18.0 |
| 2010 | 7.25 | 7.5 | 27.70 | 28.8 | 9.35 | 9.7 | 20.42 | 21.2 | 3.19 | 3.3 | 11.10 | 11.5 | 17.31 | 18.0 |
| 2015 | 6.74 | 6.2 | 31.19 | 28.5 | 10.17 | 9.3 | 26.09 | 23.9 | 4.25 | 3.9 | 11.61 | 10.6 | 19.20 | 17.6 |
| 2020 | 5.93 | 4.7 | 34.68 | 27.6 | 11.61 | 9.3 | 36.06 | 28.7 | 5.46 | 4.4 | 11.74 | 9.4 | 19.95 | 15.9 |
| 2025 | 5.66 | 4.0 | 34.44 | 24.4 | 12.69 | 9.0 | 45.24 | 32.1 | 7.18 | 5.1 | 12.57 | 8.9 | 23.14 | 16.4 |

References

- [1] UN-HABITAT. The Value of Sustainable Urbanization. 2020.
- [2] UN-HABITAT. HABITAT-INFORMAL SETTLEMENTS. Technical report, 2015.
- [3] Intergovernmental Panel on Climate Change (IPCC). IPCC Sixth Assessment Report Annex II: Glossary. Technical report, 6 2022.
- [4] World Bank 1996-2024. World Development Indicators, 2024. URL <https://databank.worldbank.org/reports.aspx?source=2&type=metadata&series=PV.PER.RNK>.
- [5] Arthur Depicker, Gerard Govers, Liesbet Jacobs, Matthias Vanmaercke, Judith Uwirirwe, Benjamin Campforts, Désiré Kubwimana, Jean Claude Mateso, Toussaint Mugaruka Bibentyo, Louis Nahimana, Benoît Smets, and Olivier Dewitte. Mobilization rates of landslides in a changing tropical environment: 60-year record over a large region of the East African Rift. *Geomorphology*, 454:109156, 6 2024. ISSN 0169-555X. doi: 10.1016/J.GEOMORPH.2024.109156. URL <https://www.sciencedirect.com/science/article/pii/S0169555X24001065?via%3Dihub>.
- [6] Antoine Dille, Olivier Dewitte, Alexander L. Handwerger, Nicolas d’Oreye, Dominique Derauw, Gloire Ganza Bamulezi, Guy Ilombe Mawe, Caroline Michellier, Jan Moeyersons, Elise Monsieurs, Toussaint Mugaruka Bibentyo, Sergey Samsonov, Benoît Smets, Matthieu Kervyn, and François Kervyn. Acceleration of a large deep-seated tropical landslide due to urbanization feedbacks. *Nature Geoscience* 2023 15:12, 15(12):1048–1055, 12 2022. ISSN 1752-0908. doi: 10.1038/s41561-022-01073-3. URL <https://www.nature.com/articles/s41561-022-01073-3>.
- [7] Arthur Depicker, Liesbet Jacobs, Nicholus Mboga, Benot Smets, Anton Van Rompaey, Moritz Lennert, Eléonore Wolff, François Kervyn, Caroline Michellier, Olivier Dewitte, and Gerard Govers. Historical dynamics of landslide risk from population and forest-cover changes in the Kivu Rift. *Nature Sustainability* 2021 4:11, 4(11):965–974, 8 2021. ISSN 2398-9629. doi: 10.1038/s41893-021-00757-9. URL <https://www.nature.com/articles/s41893-021-00757-9>.
- [8] Jean Nsabimana, Sabine Henry, Aloys Ndayisenga, Désiré Kubwimana, Olivier Dewitte, François Kervyn, Caroline Michellier, Jean Nsabimana, Sabine Henry, Aloys Ndayisenga, Désiré Kubwimana, Olivier Dewitte, François Kervyn, and Caroline Michellier. Geo-Hydrological Hazard Impacts, Vulnerability and Perception in Bujumbura (Burundi): A High-Resolution Field-Based Assessment in a Sprawling City. *Land* 2023, Vol. 12,,

- 12(10), 10 2023. ISSN 2073-445X. doi: 10.3390/LAND12101876. URL <https://www.mdpi.com/2073-445X/12/10/1876>.
- [9] Peter J. Marcotullio, Carsten Keßler, Rebeca Quintero Gonzalez, and Michael Schmeltz. Urban Growth and Heat in Tropical Climates. *Frontiers in Ecology and Evolution*, 9: 616626, 8 2021. ISSN 2296701X. doi: 10.3389/FEVO.2021.616626/BIBTEX. URL www.frontiersin.org.
- [10] Bekele Abebe, Francesco Dramis, Giandomenico Fubelli, Mohammed Umer, and Asfawossen Asrat. Landslides in the Ethiopian highlands and the Rift margins. *Journal of African Earth Sciences*, 56(4-5):131–138, 3 2010. ISSN 1464-343X. doi: 10.1016/J.JAFR.EARSCI.2009.06.006. URL <https://www.sciencedirect.com/science/article/pii/S1464343X09001113?via%3Dihub>.
- [11] Degfie Teku and Sintayehu Eshetu. Impact of climatic variabilities and extreme incidences on the physical environment, public health, and people’s livelihoods in Ethiopia. *Frontiers in Climate*, 6:1435138, 12 2024. ISSN 26249553. doi: 10.3389/FCLIM.2024.1435138/XML.
- [12] IFRC. Ethiopia Gofa Landslide Disaster Brief. Technical report, International Federation of the Red Cross, 7 2024.
- [13] GCR. Ethiopia in Crisis: Deadly Landslides and the Growing Climate Threat, 2025. URL <https://globalclimaterisks.org/insights/blog/ethiopia-in-crisis-deadly-landslides-and-the-growing-climate-threat/>.
- [14] James M. Thornton, Mark A. Snethlage, Roger Sayre, Davnah R. Urbach, Daniel Viviroli, Daniele Ehrlich, Veruska Muccione, Philippus Wester, Gregory Insarov, and Carolina Adler. Human populations in the world’s mountains: Spatio-temporal patterns and potential controls. *PLOS ONE*, 17(7):e0271466, 7 2022. ISSN 1932-6203. doi: 10.1371/JOURNAL.PONE.0271466. URL <https://journals.plos.org/plosone/article?id=10.1371/journal.pone.0271466>.
- [15] EEA. Report on the Ethiopian Economy: Economic Performance and Governance in Ethiopia. Technical report, Ethiopian Economics Association, 5 2025. URL https://eea-et.org/publication/report-on-the-ethiopian-economy-2025_economic-performance-and-governance-in-ethiopia/.
- [16] Sergio Margulis, Gordon Hughes, Robert Schneider, Kiran Pandey, Urvashi Narain, and Thomas Kemeny. Economics of adaptation to climate change: Synthesis report. Technical report, The World Bank, 2010.
- [17] Mesgana Seyoum Gizaw and Thian Yew Gan. Impact of climate change and El Niño episodes on droughts in sub-Saharan Africa. *Climate Dynamics*, 49(1):665–682, 2017. ISSN 0930-7575.
- [18] ThinkHazard. Think Hazard - Republic of Yemen - Landslide, 2025. URL <https://thinkhazard.org/en/report/269-republic-of-yemen/LS>.
- [19] Hussein Ahmed Hasan Zaid, T. A. Jamaluddin, and Mohd Hariri Arifin. Overview of slope stability, earthquakes, flash floods and expansive soil hazards in the republic of yemen. *Bulletin of the Geological Society of Malaysia*, 71:71–78, 5 2021. ISSN 01266187. doi: 10.7186/BGSM71202106.
- [20] IOM. Report on Migration, Environment and Climate Change in Yemen. Technical report, International Organization for Migration (IOM), UN Migration, 2023.

- [21] IDMC. Yemen — IDMC - Internal Displacement Monitoring Centre, 2025. URL <https://www.internal-displacement.org/countries/yemen/>.
- [22] IDMC. Global Report on Internal Displacement. Technical report, Internal Displacement Monitoring Centre, 2025.
- [23] Maxx Dilley. *Natural disaster hotspots: a global risk analysis*, volume 5. World Bank Publications, 2005. ISBN 0821359304.
- [24] Jack Rusk, Amina Maharjan, Prakash Tiwari, Tzu Hsin Karen Chen, Sara Shneiderman, Mark Turin, and Karen C. Seto. Multi-hazard susceptibility and exposure assessment of the Hindu Kush Himalaya. *Science of The Total Environment*, 804:150039, 1 2022. ISSN 0048-9697. doi: 10.1016/J.SCITOTENV.2021.150039. URL <https://www.sciencedirect.com/science/article/pii/S0048969721051147#bb0100>.
- [25] Thomas Ruttig. Slippery Slopes: Ecological, social and developmental aspects of the Badakhshan landslide disaster, 5 2014. URL <https://www.afghanistan-analysts.org/en/reports/economy-development-environment/slippery-slopes-ecological-social-and-developmental-aspects-of-the-badakhshan-landslide-disaster/>.
- [26] Alexandra Witze. Afghan landslide was 'an accident waiting to happen'. *Nature* 2014, 5 2014. ISSN 1476-4687. doi: 10.1038/nature.2014.15158. URL <https://www.nature.com/articles/nature.2014.15158>.
- [27] Hamida Salehzada, Masouda Qasimi, and Shakila Rezayi. Landslide in Badakhshan, Afghanistan, 5 2014. URL https://www.adpc.net/igo/contents/iPrepare/iprep-are-news_id.asp?ipid=250.
- [28] GFDRR. Learning from Experience Insights from China's Progress in Disaster Risk Management Learning from Experience. Technical report, The World Bank, 2020. URL www.worldbank.org.
- [29] Bin Tong, Yixiang Zhang, Gan Qi, Jusong Shi, Yuanqiang Wan, Jianyin He, and Xudong Yang. The corresponding countermeasures of landslide risk control under influence of climate change in China. *Geomatics, Natural Hazards and Risk*, 15(1), 12 2024. ISSN 19475713. doi: 10.1080/19475705.2024.2421387;WGROU:STRING:PUBLICATION. URL <https://www.tandfonline.com/doi/pdf/10.1080/19475705.2024.2421387>.
- [30] Lei Zhou, Xianhua Wu, Zhonghui Ji, and Ge Gao. Characteristic analysis of rainstorm-induced catastrophe and the countermeasures of flood hazard mitigation about Shenzhen city. *Geomatics, Natural Hazards and Risk*, 8(2):1886–1897, 12 2017. ISSN 19475713. doi: 10.1080/19475705.2017.1392368;WGROU:STRING:PUBLICATION. URL <https://www.tandfonline.com/doi/pdf/10.1080/19475705.2017.1392368>.
- [31] Ugur Ozturk, Elisa Bozzolan, Elizabeth A. Holcombe, Roopam Shukla, Francesca Pianosi, and Thorsten Wagener. How climate change and unplanned urban sprawl bring more landslides. *Nature* 2022 608:7922, 608(7922):262–265, 8 2022. ISSN 14764687. doi: 10.1038/d41586-022-02141-9. URL <https://www.nature.com/articles/d41586-022-02141-9>.
- [32] Thomas Stanley and Dalia B Kirschbaum. A heuristic approach to global landslide susceptibility mapping. *Natural hazards*, 87(1):145–164, 2017.
- [33] Laura D Triplett, Morena N Hammer, Stephen B DeLong, Karen B Gran, Carrie E Jennings, Zachary T Engle, Julie K Bartley, Dylan J Blumentritt, Andy J Breckenridge, Stephanie Day, et al. Factors influencing landslide occurrence in low-relief formerly glaciated landscapes: landslide inventory and susceptibility analysis in minnesota, usa. *Natural Hazards*, 121(10):11799–11827, 2025.